NUMERICAL SIMULATION OF A CASCADIA SUBDUCTION ZONE TSUNAMI WITH APPLICATION TO BOUNDARY BAY IN THE SOUTHERN STRAIT OF GEORGIA

Isaac Fine, Richard Thomson, and Nicky Hastings

Fisheries and Oceans Canada
Institute of Ocean Sciences
9860 West Saanich Road
Sidney, BC V8L 4B2

2023

Canadian Technical Report of Hydrography and Ocean Sciences 368

Fisheries and Oceans Canada / Pêches et Océans Canada

Canada

Canadian Technical Report of Hydrography and Ocean Sciences

Technical reports contain scientific and technical information of a type that represents a contribution to existing knowledge, but which is not normally found in the primary literature. The subject matter is generally related to programs and interests of the Oceans and Science sectors of Fisheries and Oceans Canada.

Technical reports may be cited as full publications. The correct citation appears above the abstract of each report. Each report is abstracted in the data base Aquatic Sciences and Fisheries Abstracts.

Technical reports are produced regionally but are numbered nationally. Requests for individual reports will be filled by the issuing establishment listed on the front cover and title page.

Regional and headquarters establishments of Ocean Science and Surveys ceased publication of their various report series as of December 1981. A complete listing of these publications and the last number issued under each title are published in the Canadian Journal of Fisheries and Aquatic Sciences, Volume 38: Index to Publications 1981. The current series began with Report Number 1 in January 1982.

Rapport technique canadien sur l'hydrographie et les sciences océaniques

Les rapports techniques contiennent des renseignements scientifiques et techniques qui constituent une contribution aux connaissances actuelles mais que l'on ne trouve pas normalement dans les revues scientifiques. Le sujet est généralement rattaché aux programmes et intérêts des secteurs des Océans et des Sciences de Pêches et Océans Canada.

Les rapports techniques peuvent être cités comme des publications à part entière. Le titre exact figure au-dessus du résumé de chaque rapport. Les rapports techniques sont résumés dans la base de données Résumés des sciences aquatiques et halieutiques.

Les rapports techniques sont produits à l'échelon régional, mais numérotés à l'échelon national. Les demandes de rapports seront satisfaites par l'établissement auteur dont le nom figure sur la couverture et la page de titre.

Les établissements de l’ancien secteur des Sciences et Levés océaniques dans les régions et à l'administration centrale ont cessé de publier leurs diverses séries de rapports en décembre 1981. Vous trouverez dans l'index des publications du volume 38 du Journal canadien des sciences halieutiques et aquatiques, la liste de ces publications ainsi que le dernier numéro paru dans chaque catégorie. La nouvelle série a commencé avec la publication du rapport numéro 1 en janvier 1982.

Canadian Technical Report of
Hydrography and Ocean Sciences 368

2023

NUMERICAL SIMULATION OF A CASCADIA SUBDUCTION ZONE TSUNAMI WITH APPLICATION TO BOUNDARY BAY IN THE SOUTHERN STRAIT OF GEORGIA

Isaac Fine[1], Richard Thomson[1], and Nicky Hastings[2]

[1]Fisheries and Oceans Canada
Institute of Ocean Sciences
9860 West Saanich Road
Sidney, BC V8L 4B2

[2]Natural Resources Canada
Geological Survey of Canada - Pacific Division
605 Robson Street
Vancouver, BC V6B 5J3

Cat. No.: Fs97-18/368E-PDF ISBN 978-0-660-68787-2 ISSN 1488-5417

Correct citation for this publication:

Fine, I., Thomson, R., and Hastings, N., 2023. Numerical simulation of a Cascadia Subduction Zone tsunami with application to Boundary Bay in the southern Strait of Georgia. Can. Tech. Rep. Hydrogr. Ocean Sci. 368: v + 39 p.

CONTENTS

1 INTRODUCTION 1

2 NUMERICAL TSUNAMI MODEL 2

2.1 Model Setup: Nested Grid Formulation 2

2.1.1 Coarse Grid (Grid 1) 4

2.1.2 Intermediate Grid (Grid 2) 4

2.1.3 Intermediate Grid (Grid 3) 7

2.1.4 Final Grid (Grid 4) 8

2.2 Model Reference Levels 10

2.3 The Source Distribution 11

3 RESULTS 13

3.1 Comparison of modelled tsunami waves for two CSZ scenarios for coarse and intermediate grids 13

3.2 Detailed Results for Boundary Bay: Variations of Sea Levels and Tsunami-induced Currents 16

4 SUMMARY AND CONCLUSIONS 35

ACKNOWLEDGEMENTS 37

REFERENCES 38

ABSTRACT

Fine, I., Thomson, R., and Hastings, N., 2023. Numerical simulation of a Cascadia Subduction Zone tsunami with application to Boundary Bay in the southern Strait of Georgia. Can. Tech. Rep. Hydrogr. Ocean Sci. 368: v + 39 p.

A high-resolution, four-level, nested-grid tsunami model was used to simulate tsunami waves and wave-induced currents that will be generated in Boundary Bay in the southern Strait of Georgia by a Cascadia Subduction Zone earthquake with magnitude M_w 9.0. Two versions of the earthquake-induced tsunami source region were used: Model A, a whole margin buried rupture; and Model B, a whole margin splay-faulting rupture. We found that the two models produce similar results, with Model A generating slightly higher wave amplitudes in the Bay. For both models, the first wave to arrive is a wave trough of 60-80 cm. The leading wave crest that follows the trough is the highest wave, with a peak of 1.1-1.5 m, and arrives roughly 2:45 – 3:15 hours after the start of the earthquake. The primary period of the tsunami waves is 2-3 hours. Maximum wave amplitudes (of up to 1.5 m) occur within the north-western part on the Bay, and along the Semiahmoo coast (up to 1.3 m). The tsunami-induced ocean currents are typically less than 1 m/s in most areas but are up to 3 m/s at the entrance to Drayton Harbor and up to 2 m/s at the mouth of Campbell River on the Semiahmoo coast. Tsunami waves would cause flooding in coastal areas but will be restricted by the presence of the elongated dike. Flooding in the Semiahmoo area will likely occur in the Campbell River valley but will have a limited effect.

RÉSUMÉ

Fine, I., Thomson, R., and Hastings, N., 2023. Numerical simulation of a Cascadia Subduction Zone tsunami with application to Boundary Bay in the southern Strait of Georgia. Can. Tech. Rep. Hydrogr. Ocean Sci. 368: v + 39 p.

Un modèle de tsunami à haute résolution, à quatre niveaux et à grille imbriquée, a été utilisé pour simuler les vagues de tsunami et les courants induits par les vagues qui seront générés à Boundary Bay, dans le sud du détroit de Géorgie, par un tremblement de terre dans la zone de subduction de Cascadia d'une magnitude M_w 9,0. Deux versions de la région source du tsunami provoqué par le séisme ont été utilisées : le modèle A, une rupture enfouie sur toute la marge ; et le modèle B, une rupture de faille sur toute la marge. Nous avons constaté que les deux modèles produisent des résultats similaires, le modèle A générant des amplitudes de vagues légèrement plus élevées dans la baie. Pour les deux modèles, la première vague à arriver est un creux de vague de 60 à 80 cm. La crête de vague principale qui suit le creux est la vague la plus haute, avec un pic de 1,1 à 1,5 m, et arrive environ 2 h 45 à 3 h 15 après le début du séisme. La période principale des vagues du tsunami est de 2 à 3 heures. Les amplitudes maximales des vagues (jusqu'à 1,5 m) se produisent dans la partie nord-ouest de la baie et le long de la côte de Semiahmoo (jusqu'à 1,3 m). Les courants océaniques induits par le tsunami sont généralement inférieurs à 1 m/s dans la plupart des zones, mais peuvent atteindre 3 m/s à l'entrée du port de Drayton et jusqu'à 2 m/s à l'embouchure de Campbell River, sur la côte de Semiahmoo. Les vagues du tsunami provoqueraient des inondations dans les zones côtières mais seraient limitées par la présence de la digue allongée. Les inondations dans la région de Semiahmoo se produiront probablement dans la vallée de la rivière Campbell, mais auront un effet limité.

1. INTRODUCTION

The coast of British Columbia is susceptible to tsunamis generated by tsunamigenic earthquakes throughout the Pacific Ocean. The catastrophic tsunamis of the last two decades, including the 2004 Sumatra, 2010 Chile and 2011 Tohoku events, highlight the serious threat that major seismically generated tsunamis pose to coastal communities in southern British Columbia. Estimations of the potential tsunami risk to the British Columbia coast from events similar to the magnitude M_w 9.2 Alaska earthquake and tsunami of March 1964 and the magnitude M_w 9.0 Cascadia Subduction Zone (CSZ) earthquake and tsunami of January 1700 are of considerable importance to broad, low-lying areas of British Columbia, such as Boundary Bay in the southern Strait of Georgia. This risk is expected to increase as sea levels continue to rise through the effects of global warming.

The objective of this study was to simulate seismically generated tsunamis arriving at Boundary Bay in the southern Strait of Georgia from a major magnitude M_w 9.0 earthquake along the Cascadia Subduction Zone, similar to the historical event of January 1700. Accurate simulation of tsunami waves propagating into this rapidly shoaling region of the west coast of British Columbia from the open ocean requires a series of nested bathymetric sub-grids of ever finer spatial and temporal resolution. The use of nested numerical grids of ever smaller grid-cell dimension and time steps makes it possible to better resolve tsunami wave properties in shallow coastal regions such as Boundary Bay and the lands of the Semiahmoo First Nation on the eastern side of the bay.

2. NUMERICAL TSUNAMI MODEL

2.1. MODEL SETUP: NESTED GRID FORMULATION

Accurate numerical simulation of tsunami waves in the rapidly shoaling regions of the west coast of British Columbia requires setting up the model domain as a series of nested grids of ever finer spatial and temporal resolution. The use of nested grids of smaller cell dimensions and time steps makes it possible to resolve tsunami wave configurations as they propagate into the shallow coastal regions. The principal requirements for numerical models using nested grids are as follows:

- Nested grid cell sizes are generally obtained by dividing the initial, large-scale coarse numerical grid by an integer, typically 3 to 5. Integers larger than this can lead to grid interface problems;
- Nested grids are needed in near-coastal areas; the coarse “parent” grid should be of sufficient extent to resolve possible feed-back effects that the nested grid may have on the parent grid during the simulation time;
- A good interface between the inner and outer domains is required to avoid errors and model instability associated with point matching between the different grids. This should allow two-way fluxes without trapping shorter waves at the inner domain boundaries;

- High resolution bathymetry, external forcing and observations are needed for model domain setup, initialization and validation at each domain level; here the nested-grid formulation is similar to that used in well-known tsunami models, TUNAMI and COMCOT (Liu *et al.*, 1998; Imamura, *et al.*, 2006).

Because of the relatively long periods of the tsunamis generated in the deepwater source regions used in this study, and because of the relatively short propagation times of 2 to 3 hours between the source region and the Boundary Bay, the dispersion effect is negligible. In this case, high bathymetric resolution is the important factor for modelling wave propagation in the offshore regions.

Table 1. Parameters of the numerical grids used in the tsunami generation and propagation model. Grid extent is along the *x* (eastward) and *y* (northward) coordinate directions and is presented in degrees (°). Numerical grid cell sizes for Grids 2, 3 and 4 are roughly 270, 60 and 10 m, respectively. Columns 2,3 and 4 are presented as *x*, *y* values.

Grid No.	Extent (*x*, *y*) (degrees)	Array (number of grid points)	Cell size (degrees)	Source of data	Processing type
1	18.0, 17.0	721,1021	0.025, 0.01667	GEBCO 2014 30 arc-seconds gridded data	Filtering and bilinear interpolation
2	6.595, 4.2	1261,1520	0.005, 0.00333	BC 3 arc-sec bathymetric DEM	Filtering and bilinear interpolation
3	0.74, 0.55	811, 889	0.0008333, 0.0005555	BB 1/9 arc second DEM,	Filtering and interpolation
4	0.38, 0.20	2737, 2161	0.000138889, 0.0000925926	BB 1/9 arc second,	Filtering and interpolation

The present project uses a series of four nested grids for the Cascadia Subduction Zone (CSZ) tsunami model (Table 1). The choice of model grids takes into account the need for high spatial resolution to accurately resolve the reflection and transformation of the waves and the need for large spatial extent to capture full source area.

2.1.1. Coarse grid (Grid 1)

Grid 1 is the coarsest numerical grid used in the model. This large-scale grid covers the northeast Pacific and encompasses the major source region used in the simulations for the CSZ (Figure 1). The northeast Pacific is an important tsunami wave generation region through which all offshore tsunamis propagate on their way to coastal British Columbia. The grid was created using the 30 arc-second global bathymetry dataset GEBCO2014 (GEBCO, 2014).

The spatial resolution of the coarse grid is 90 arc-seconds in the east-west (x) direction (spatial scales ranging from 1.4 km to 2.2 km, depending on latitude) and 60 arc-seconds in the north-south (y) direction (1.85 km grid size). The grid is bounded by 38– 55° N, 140 – 122° W. A typical spatial scale for each grid cell is thus about 1.8 km.

2.1.2. Intermediate grid (Grid 2)

Grid 2 covers water surrounding Vancouver Island, British Columbia and the northwest US coast (Figure 2). The location and coverage of the grid was chosen so that it covered all passes into the Strait of Georgia. This intermediate grid is important for simulating wave transformation as the tsunami enters the Salish Sea through Juan de Fuca Strait. This grid is also important for tsunamis penetrating into the Strait of Georgia through narrow straits, capturing the energy exchange between the deeper shelf waters and the much shallower coastal zone.

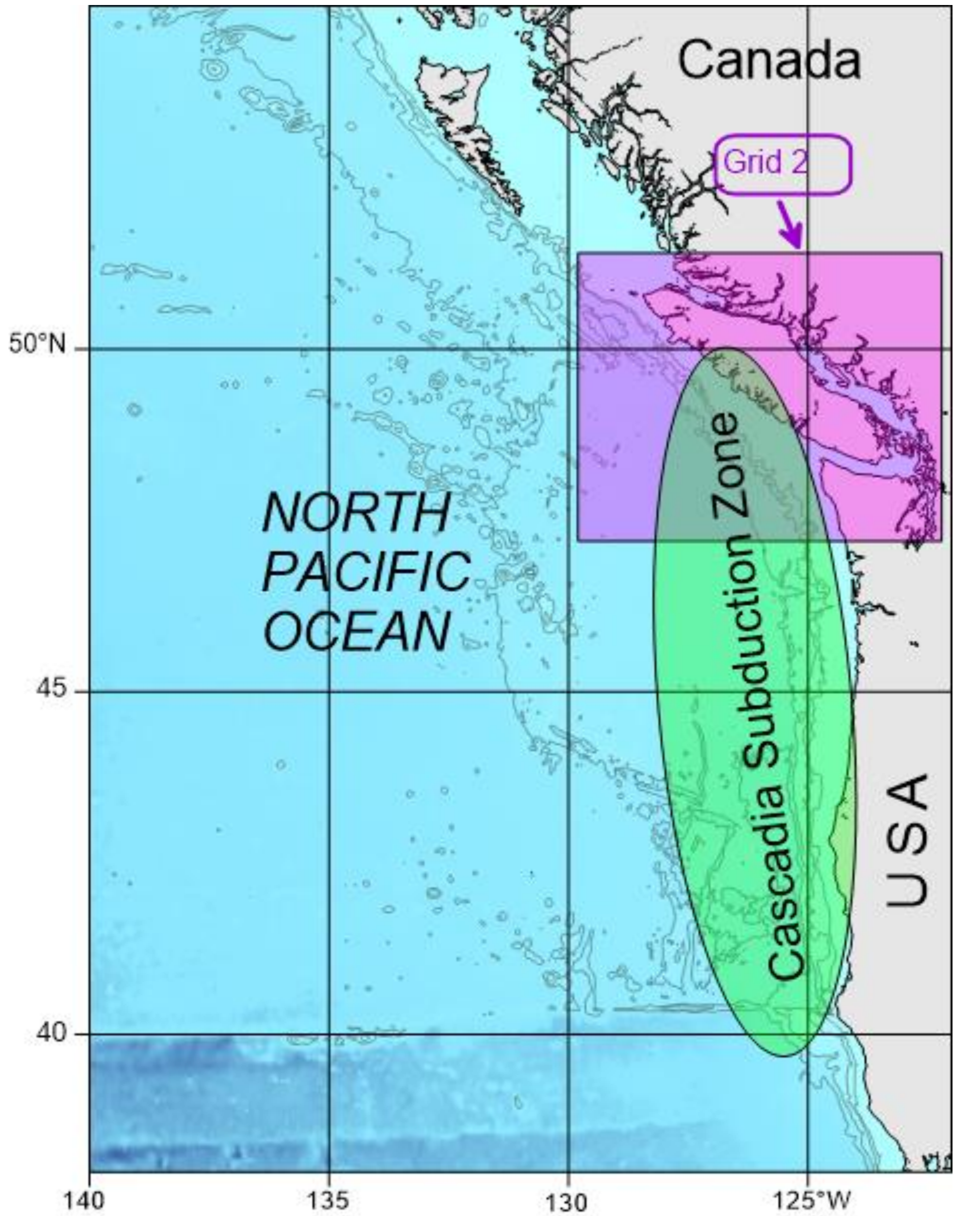

Figure 1. The region covered by the large-scale coarse grid numerical model for the northeast Pacific (Grid 1). Also shown is the Cascadia Subduction Zone where a tsunami could be generated that would impact the Boundary Bay area. The insert shows the location of the first nested grid (Grid 2), covering the southwest coast of British Columbia and northwest Washington State.

The grid was created using the British Columbia 3 arc-second bathymetric Digital Elevation Model (DEM), (NOAA, 2017). Grid 2 has a resolution of 18 arc-seconds in the east-west direction and 12 arc-seconds in the north-south direction, corresponding to spatial scales (x, *y*) of approximately 370 m and 370 m, respectively (Table 1). The grid boundaries span 47.2°–51.4°N, 129.8° – 122.2°W.

To comply with the Grid 3 bathymetry (see 1.1.3), we also replaced the Boundary Bay area data of Grid 2 with data computed with a high-resolution digital model for Boundary Bay; the original 3-arc second data in that area are too inaccurate for that region.

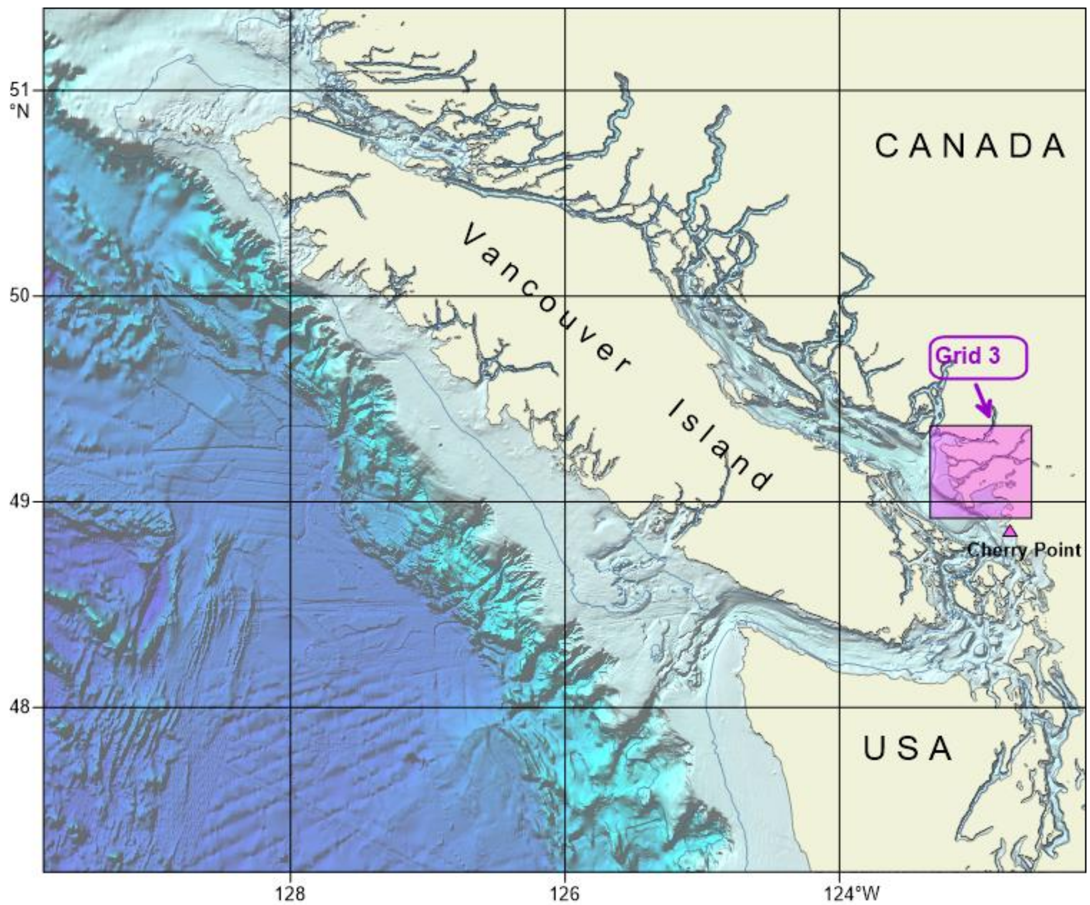

Figure 2. Vancouver Island and surrounding oceanic regions covered by the medium-scale bathymetric grid (Grid 2) for the southwest coast of British Columbia. The horizontal grid cell scales (*x*, *y*) for this region are approximately 370 m. The insert shows the boundaries and location of the second nested grid (Grid 3) covering the region of Vancouver and Boundary Bay.

2.1.3. Intermediate grid (Grid 3)

The third numerical grid covers the waters surrounding Metro Vancouver. (Figure 3). This grid is of considerable importance since it determines wave transformation in the vicinity of Boundary Bay. Model grid cells were created using the 1/9 arc-second Boundary Bay digital Elevation Model (BBDEM, 2020). The gridded data were subsequently re-interpolated to a geographical coordinate system (NAD83 standard) with a rectangular grid cell size of 3 arc-seconds by 2 arc-seconds (approximately 61 m by 62 m) in the east-west and north-south directions, respectively.

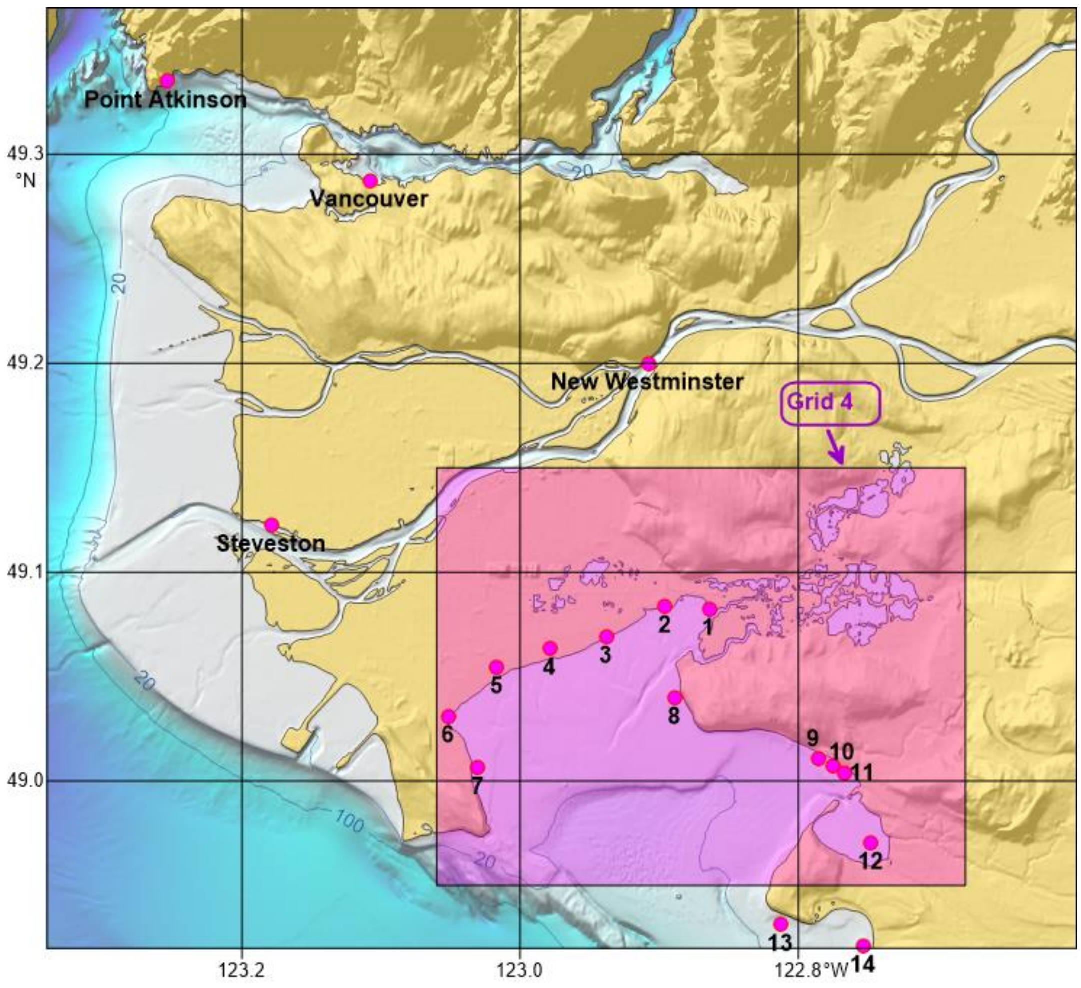

Figure 3. The coastal region covered by Grid 3, including the waters surrounding Greater (Metro) Vancouver. The *x*, *y* grid scales for this region are approximately 61 m and 62 m, respectively. Shown are the locations of the tide gauges (solid dots) and the modelled sites (numbers 1-14). The area above mean sea level is shaded yellow. The insert shows the boundaries and location of the fourth nested grid (Grid 4) covering Boundary Bay.

2.1.4. Final grid (Grid 4)

The final (fourth) numerical grid has the highest spatial resolution and covers Boundary Bay (Figure 4). The grid has been created specifically for the Boundary Bay area and is designed for estimation of tsunami inundation and tsunami-induced currents.

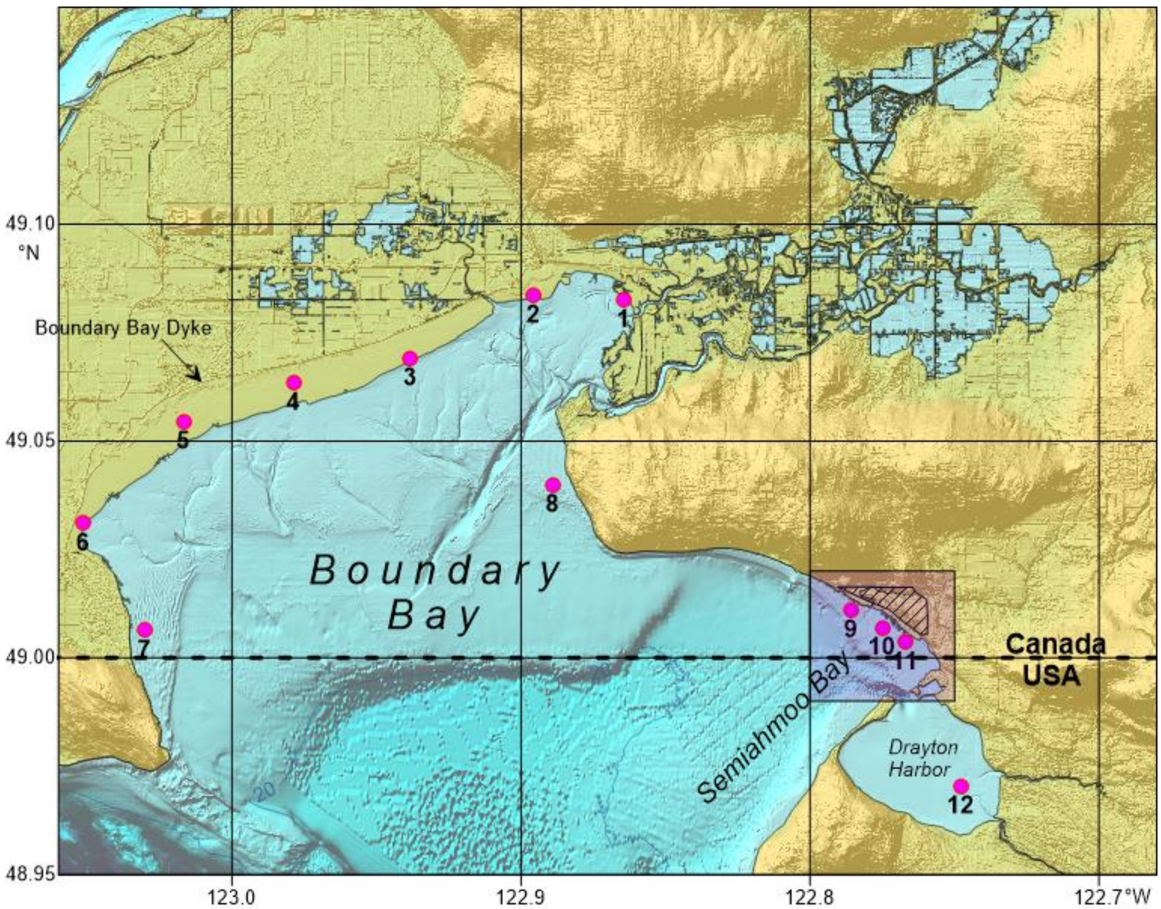

Figure 4. The region covered by Grid 4. The fine-scale bathymetric grid has adjusted topography for Boundary Bay, with grid scales (x, y) of approximately 10 m by 10 m. Also shown are the sites (numbers 1-12) in Boundary Bay for which tsunami wave records have been simulated. Depths, H, are in metres (m). The area above mean sea level is shaded in yellow. The hatched area denotes the location of the Semiahmoo, First Nation Reserve.

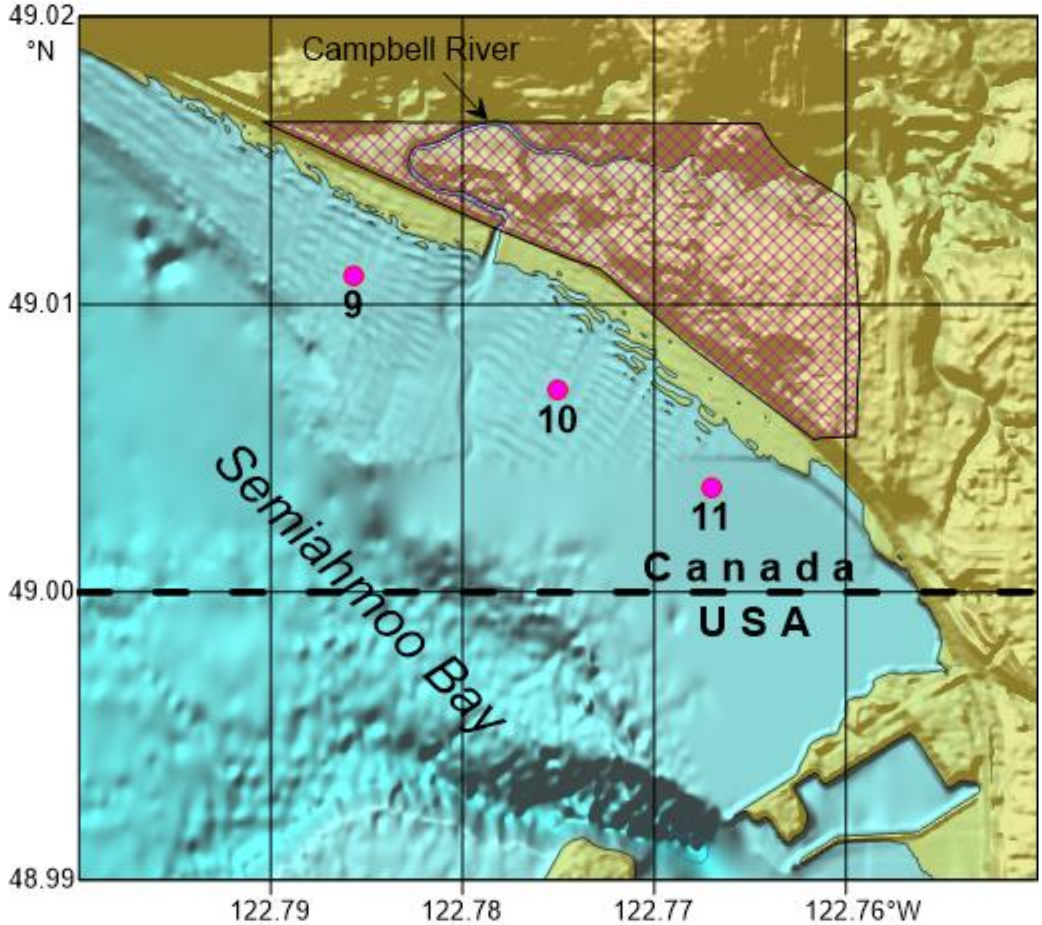

Figure 5. A fragment of the area covered by Grid 4, surrounding the Semiahmoo First Nation Reserve (shaded by a mesh). Also shown are locations of the sites (9-11) for which tsunami wave records have been simulated. The area above mean sea level is shaded in yellow.

2.2. MODEL REFERENCE LEVEL

Model simulations are generally conducted for tsunami arrival times that coincide with times of Canadian Vertical Datum of higher high water mean tide (HHWMT). The National Tsunami Hazard Mapping Program of 2010 (Nikolsky et al., 2013) recommends that inundation maps be computed using high tide as the initial condition for modelling. Alaska University uses Mean Higher High Water (MHHW) as the initial condition (Suleimani et al., 2013), while Washington State inundation map was created using Mean High Water (MHW) for initial conditions (Eungard et al., 2018. The Canadian standard HHWMT is close to the US standard MHHW, and has been used for many tsunami modelling projects in BC for Victoria (AECOM, 2013) for Victoria and Seal Cove (Fine et al., 2018a, 2018b), and for Prince Rupert (The City of Prince Rupert Tsunami Flooding Risk Assessment, 2019). Accordingly, to present values of highest risk, maps of maximum tsunami wave amplitude (~½ trough to crest wave height) and current speed in this report are referenced to HHMWT rather than to the mean tide or to a geodetic reference.

Higher High Water Mean Tide (HHWMT) is used as the primary reference level for most modelling results. For the Boundary Bay area, the closest permanent tide gauges are at Point Atkinson and Vancouver (Canadian Hydrographic Services) to the north and Cherry Point (NOAA) to the south. HHWMT is 1.30 m above Mean Sea Level (MSL) at Point Atkinson and 1.32 m above MSL at Vancouver; in comparison, MHHW used in the US is 1.18 m above MSL at Point Atkinson (see Table 2 below). For convenience, a common reference value of 1.2 m is added throughout the region for the tsunami modelling. Mean Sea Level (MSL) is 0.18-0.19 m above the Canadian geodetic datum CVD2013 (Table 2).

However, when examining the waves themselves, the wave displacement, h, presented in the figures can be considered as the wave crest amplitude measured relative to the tide level at the time of the tsunami arrival. This has a positive value. Sometimes, we want to show the depth of the wave trough, in which case “amplitude” will have a negative value measured downward from the tide level at the time of the tsunami.

Table 2. Vertical datum values for tidal stations provided by the Canadian Hydrographic Service and NOAA (USA). Latitude and longitude are in degrees and minutes. Mean Higher High Water (MHHW) and Mean Lower Low Water (MLLW) are defined in two ways: (1) in Canada using tidal predictions derived from tide gauge records; and (2) in the United States using observations from USA tide gauges. All values are referenced to Mean Sea Level (MSL), which by definition in this study is then zero (0.0). Here, CGVD 2013 denotes the Canadian Geodetic Vertical Datum.

Tide gauge ID	Name	Latitude (°N)		Longitude (°W)		CGVD 2013	MSL	MHHW	MLLW
		Deg	Min	Deg	Min	(m)	(m)	(m)	(m)
7795	Point Atkinson	49	20.25	123	22.42	-0.193	0.0	1.30	-1.94
7735	Vancouver	49	17.23	123	6.587	-0.18	0.0	1.32	-1.96
9449424	Cherry Point	48	51.8	122	45.5	-	0.0	1.18	-1.61

2.3 TSUNAMI SOURCE DISTRIBUTIONS

Based on recent advances in Cascadia tsunami source development (cf. Wang and Tréhu, 2016), we considered two different CSZ earthquake source models for tsunamis impacting the coast of British Columbia: Model A, the "buried" model; and Model B, the "splay" model (Figure 5). The models correspond to the same seismic momentum magnitude (M_w = 9.0) but to different cross-shore distributions of the associated seismic seafloor uplifts, h_0. The models are based on the northward extensions from the Witter et al. (2013) seismic sources off California to Washington, but also include source areas located to the west of Vancouver Island.

The splay-faulting rupture model includes a contribution of coseismic horizontal displacements to the initial tsunami wave field through a component of ocean surface uplift due to the horizontal motion of the steep ocean bottom slopes (Gao, 2016). Numerical tsunami simulations reveal that including the deformation due to horizontal displacements in the source function, results in an increase in the far-field tsunami amplitudes. The resulting coseismic vertical deformations (h_0) are shown in Figure 5.

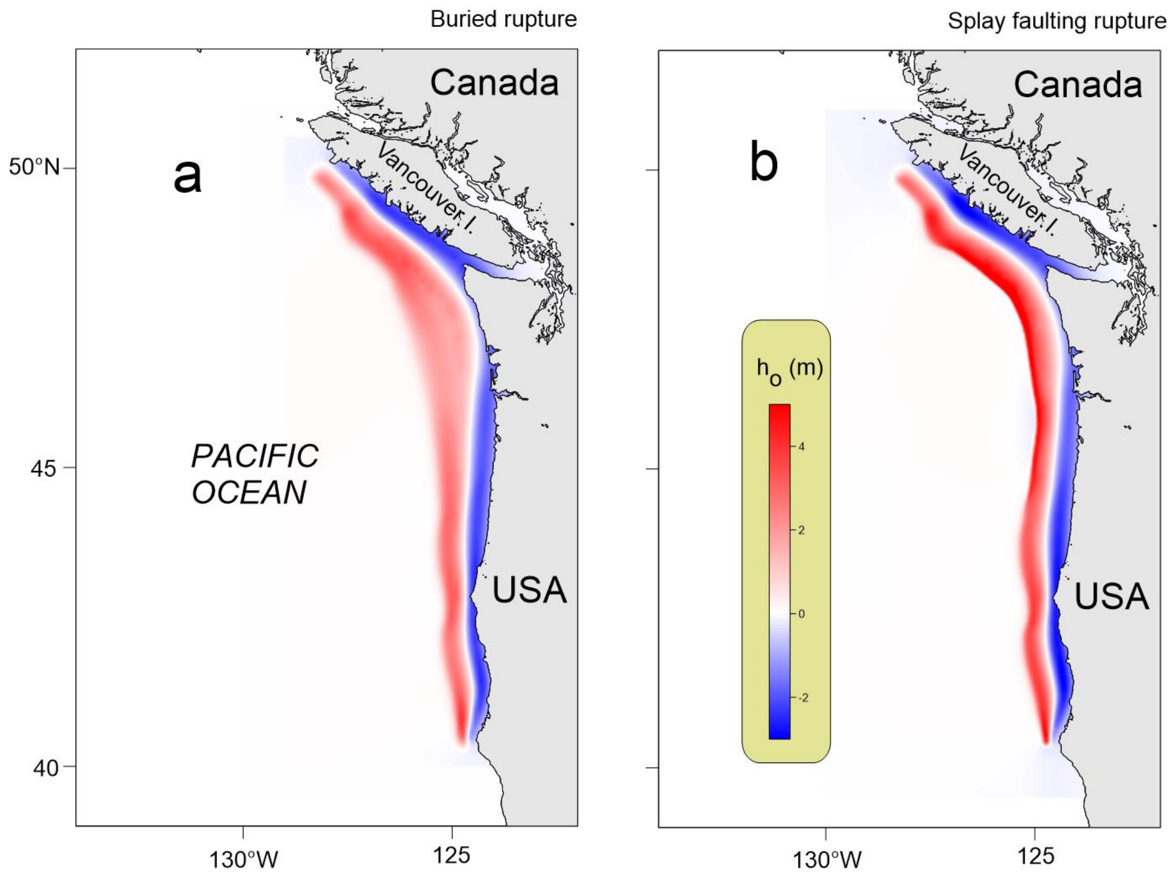

Figure 6. Maps of the Cascadia rupture zone tsunami sources according to Gao (2016). Seafloor displacements, h_0, are in metres. (a) Whole margin buried rupture (Model A); and (b) Whole margin splay-faulting rupture (Model B).

Model A is the case when the source deformation slip is located well below the sea bed, whereby the seafloor uplift has a smooth and gentle cross-shore profile, with a maximum uplift of 4 m. Model B corresponds to the "splay" model, where the rapture edges are at the seafloor. This model corresponds to the case "M1" in the (Witter et al., 2013) classification and can be considered the most probable scenario. Maximum uplift is near 8 m. We note that the two previous models for Cascadia tsunami sources for the BC coast, (Cherniawsky et al., 2007) and (AECOM, 2013), used tsunami sources that are somewhere between Models A and B.

3. RESULTS

3.1. COMPARISON OF MODELLED TSUNAMI WAVES FOR TWO CSZ SCENARIOS FOR COARSE AND INTERMEDIATE GRIDS

Figure 7 presents the results for the CSZ tsunami simulations for the coarse, open-ocean grids for Model A and Model B. As these models indicate, maps of the tsunami amplitude maxima (wave crest maxima) for the open ocean are quite different: Model B provides much more intensive waves, with stronger interference of waves arriving from the northern and southern sectors of the CSZ. Waves generated by the splay faulting rupture (Model B) have a stronger impact on coastal areas of Vancouver Island and the US west coast than waves generated by the buried rupture (Model A).

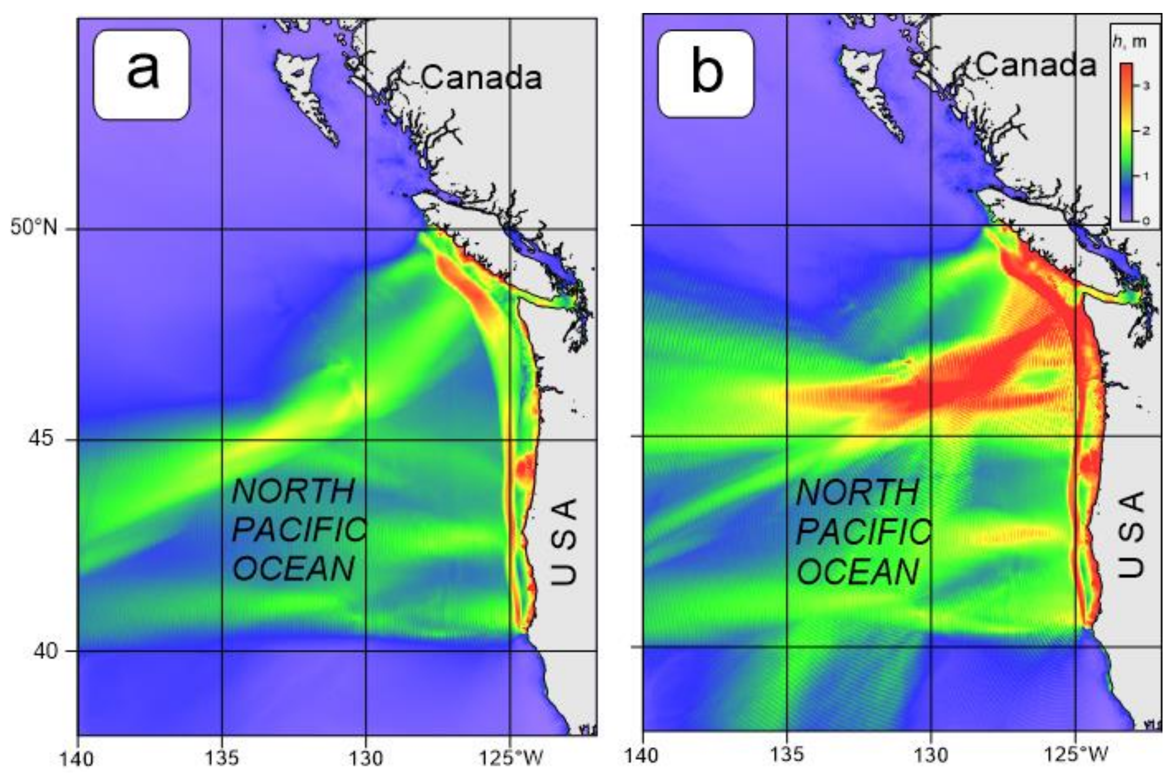

Figure 7. Spatial distribution of maximum tsunami wave amplitudes (*h*, in metres) for Grid 1 of the nested-grid model for waves generated by simulation of the CSZ tsunami for (a) Model A; and (b) Model B.

For the area around Vancouver Island (Grid 2, Figure 8), the differences between the results for models A and B do not follow a simple pattern. In general, Model B estimates higher wave displacements than Model A at the shelf areas and at the entrance and central part of Juan de Fuca Strait. At the eastern end of Juan de Fuca Strait and throughout the Strait of Georgia, the amplitudes of the tsunami waves for Model A and Model B are similar.

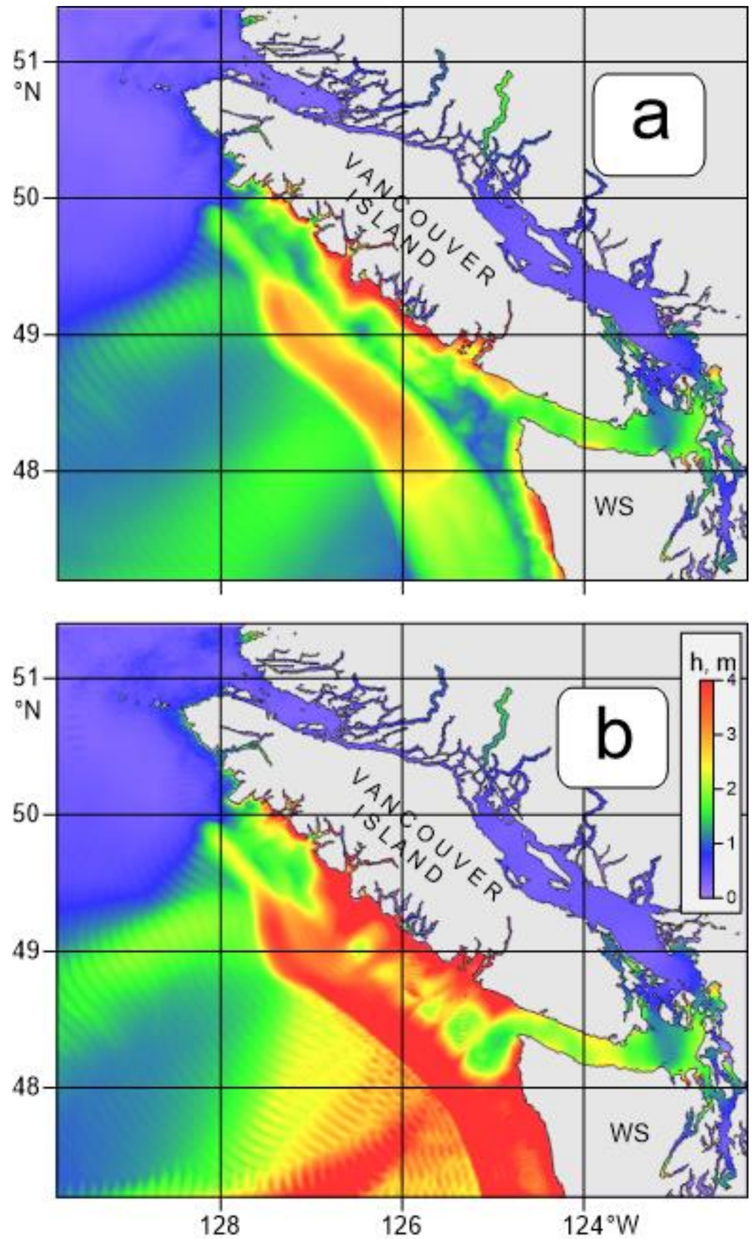

Figure 8. Spatial distribution of maximum tsunami wave amplitudes (*h*, in metres) for Grid 2 of the nested-grid model for waves generated by simulation of the CSZ tsunami for (a) Model A; and (b) Model B.

Figure 9 shows the higher resolution Model A and B results for Grid 3, which covers the approach Boundary Bay and the waters surrounding Metro Vancouver. The tsunami waves in Boundary Bay have amplitudes of up to 1.5 m, which is significantly higher than the wave amplitudes adjacent to Metro Vancouver, where they are typically around 0.5 m. Also, tsunami amplitudes are increased toward the coast in most areas. The resultant tsunami waves are slightly (approximately, 2 to 7%) higher for Model A than for Model B.

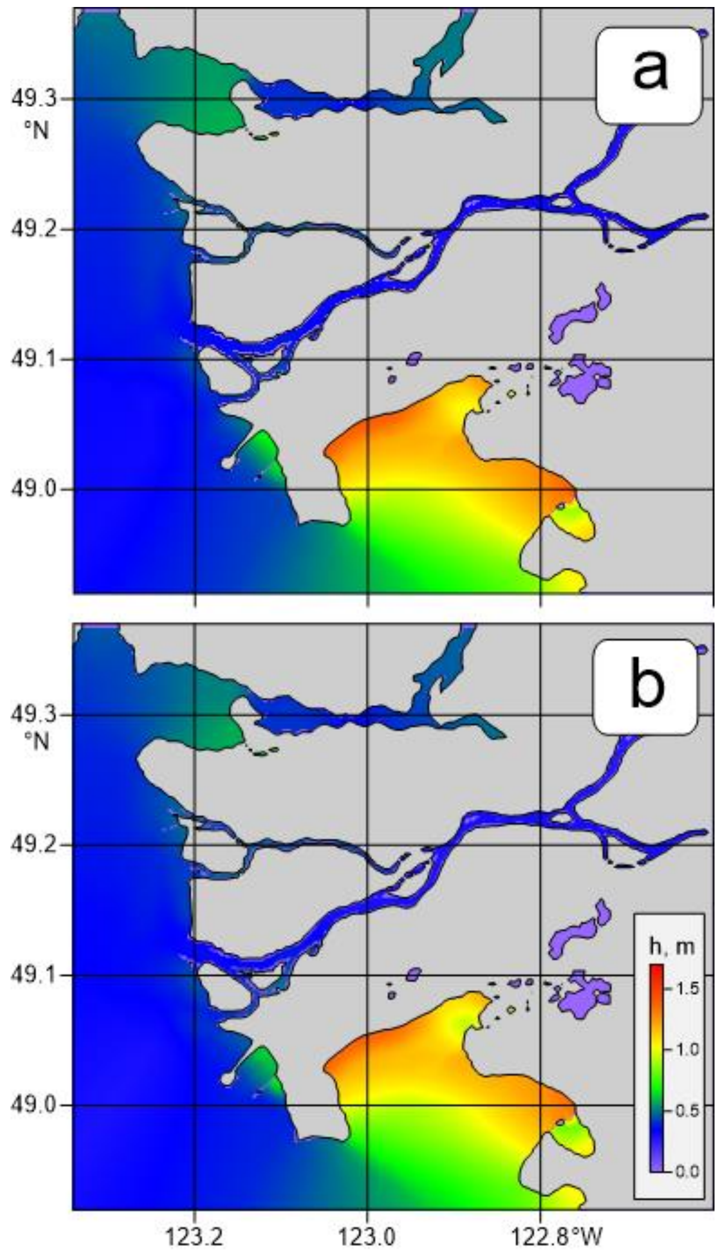

Figure 9. Spatial distribution of maximum tsunami wave amplitudes (*h*, in metres) for Grid 3 of the nested-grid model for waves generated by simulation of the CSZ tsunami for (a) Model A and (b) Model B.

3.2. DETAILED RESULTS FOR BOUNDARY BAY: TSUNAMI-INDUCED VARIATIONS IN SEA LEVEL AND CURRENTS

Detailed distributions of the maximum wave amplitudes and wave-induced currents in Boundary Bay are presented in Figures 10-13. According to Figure 10, the maximum tsunami amplitudes in Boundary Bay are around 1-1.4 m for both models. The spatial amplitude distributions are quite similar for both cases, but wave amplitudes for Model A are 3-5% higher than those for Model A. Inside Boundary Bay, the highest tsunami waves would occur at the north-western part of the bay and along the coast of Semiahmoo Village (up to 1.3-1.4 m).

Figure 11 shows the distribution of the tsunami waves along at the coast of Semiahmoo. It is clear that the distribution is nearly uniform, with a slight increase toward the south end of the Semiahmoo coast. The waves penetrate into Campbell River, but with smaller amplitudes (1-1.2 m). Wave amplitudes decrease with propagation up to the river.

The tsunami-induced currents are strong in in some specific places, like at the entrance to Drayton Harbor (Figure 12) where they can reach 3 m/s (6 knots). In most of other areas, the tsunami-induced current does not exceed 1-1.5 m/s (2-3 knots). The spatial distributions of the currents for both models are similar.

A detailed distribution of the tsunami-induced current on the Semiahmoo Coast is shown in Figure 13. The strongest currents are found at the river mouth (up to 1.5-2 m/s, or 3-4 knots for both models). In all other regions, the current is much weaker, typically not exceeding 0.5 m/s. The tsunami-induced currents are slightly stronger for Model B than current in Model A, which relates to the larger contribution of high-frequency energy in Model B compared to Model A.

Figures 14, 15 shows maps of the inundation areas for both models. It is evident that inundation areas are limited to the northwest part of Boundary Bay, where waves are blocked by the dike located around the northern part of the Bay (see Figure 4). The dike has a typical elevation of 3.5 m above MSL and is, therefore, everywhere higher than high tide plus the tsunami wave amplitude, although the available “free-board” (the spare amplitude to the top of the Boundary Bay Dyke) is only about 1 m. On the Semiahmoo coast (Figure 15), waves are unlikely to overtop the coastal road but could flood some areas at the mouth of Campbell River and up to the river valley.

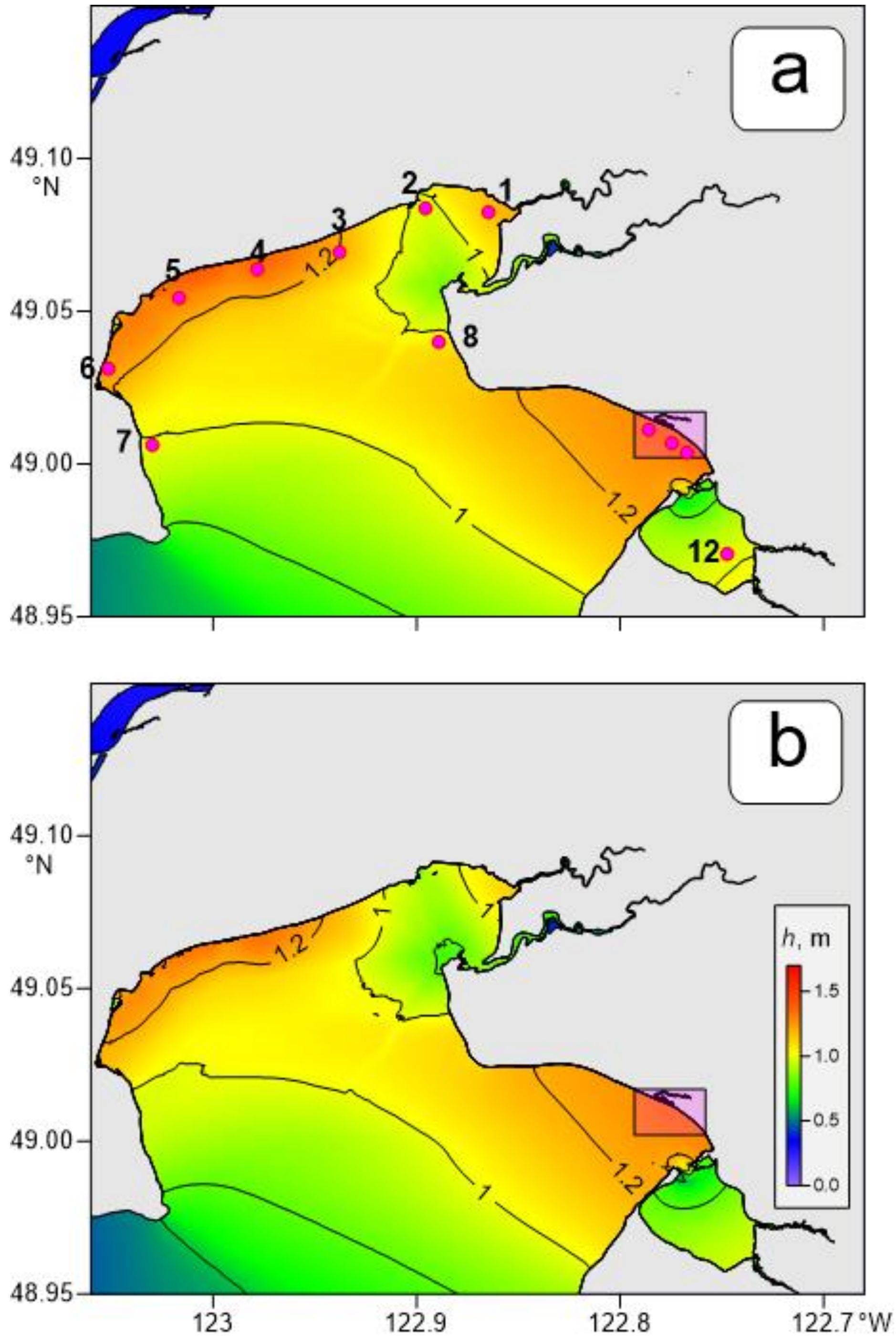

Figure 10. Distribution of maximum CSZ tsunami wave amplitudes (*h*, m) from Grid 4 in Boundary Bay for (a) Model A and (b) Model B. Numbers in Boundary Bay denote sites for which tsunami wave records have been simulated.

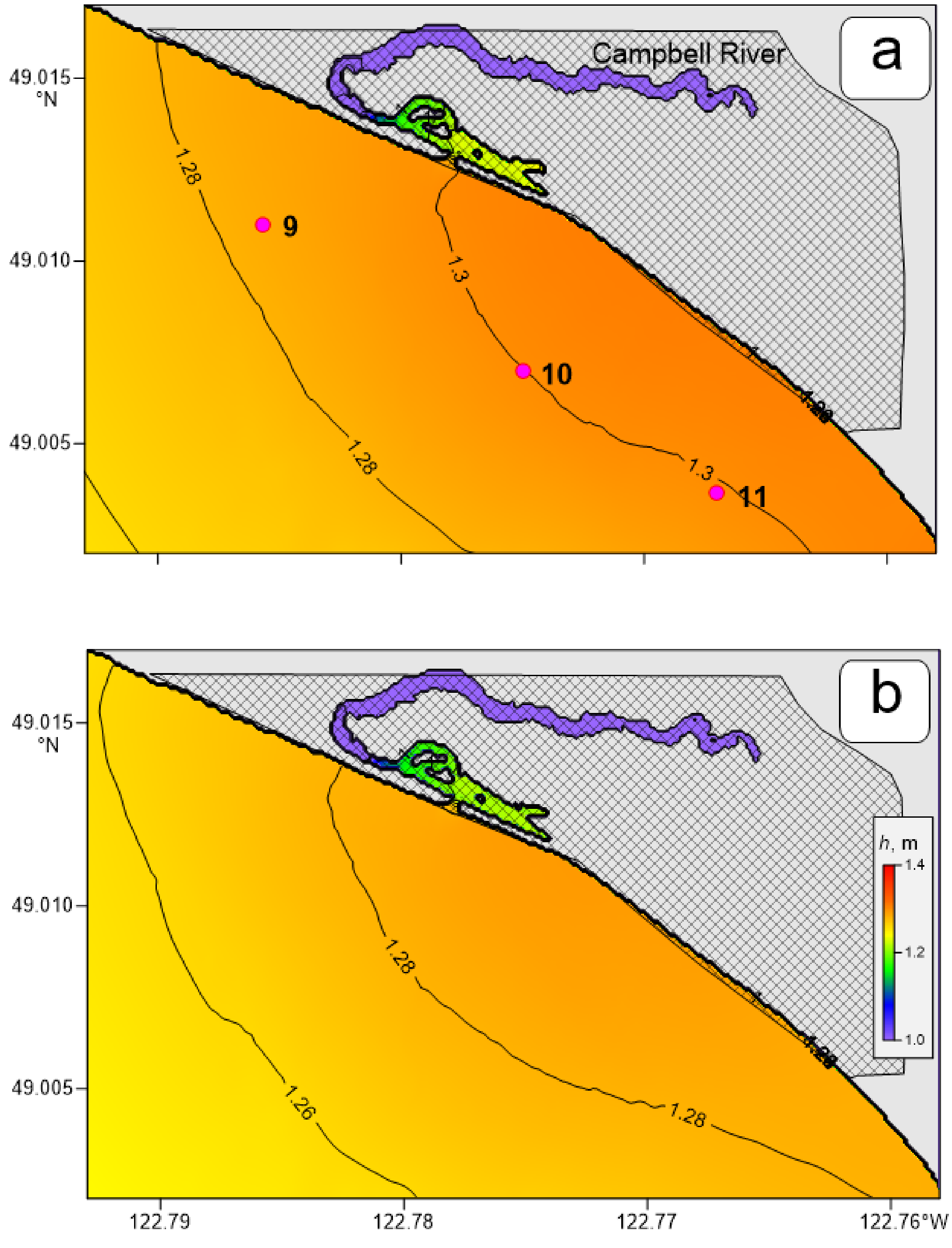

Figure 11. Distribution of maximum CSZ tsunami wave amplitudes (*h*, m) on the Semiahmoo coast for (a) Model A and (b) Model B. Numbers denote sites for which tsunami wave records have been simulated.

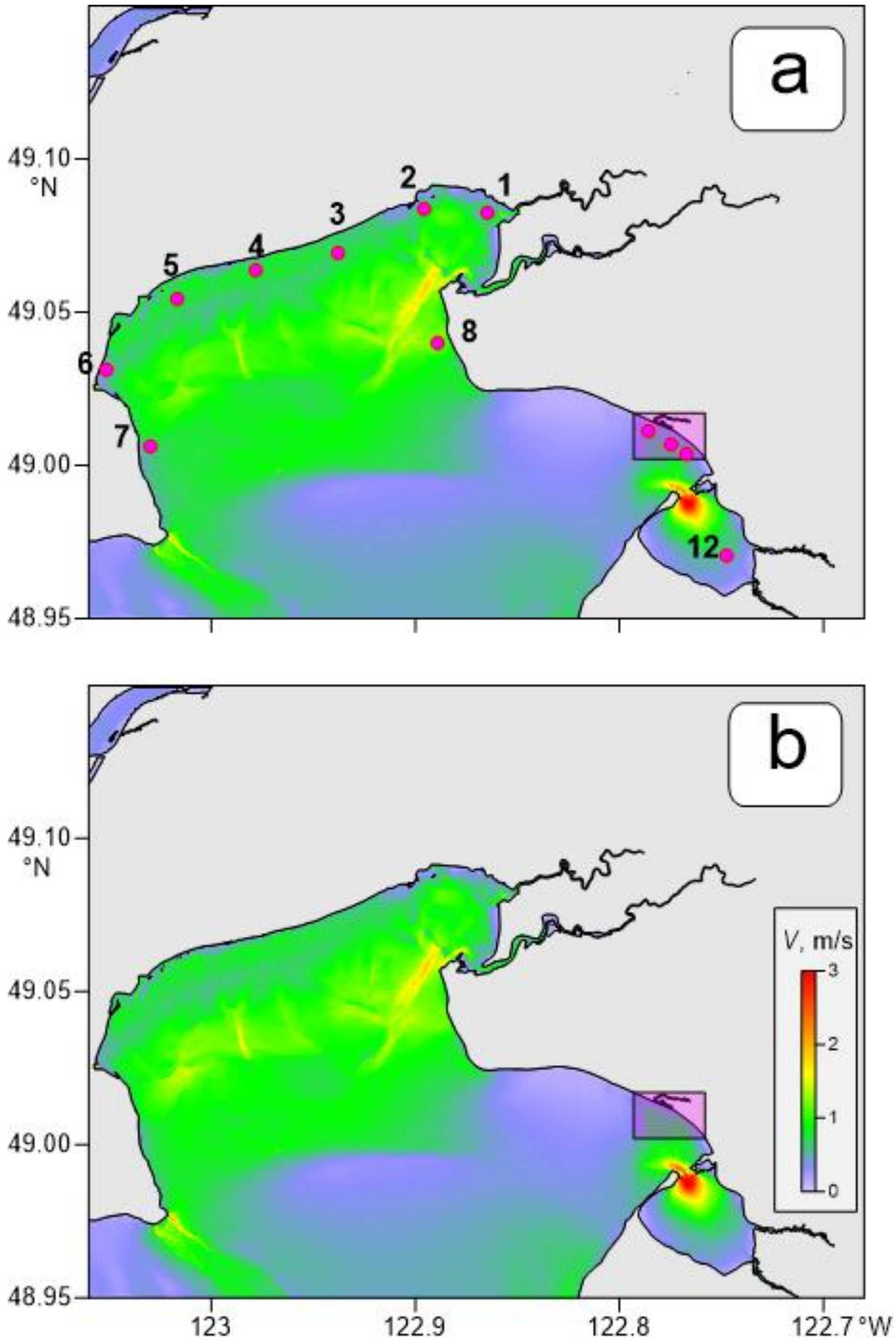

Figure 12. Distribution of the maximum CSZ tsunami-induced currents (*V*, m/s) for Grid 4 in Boundary Bay for (a) Model A and (b) Model B. Numbers denote sites for which tsunami wave records have been simulated.

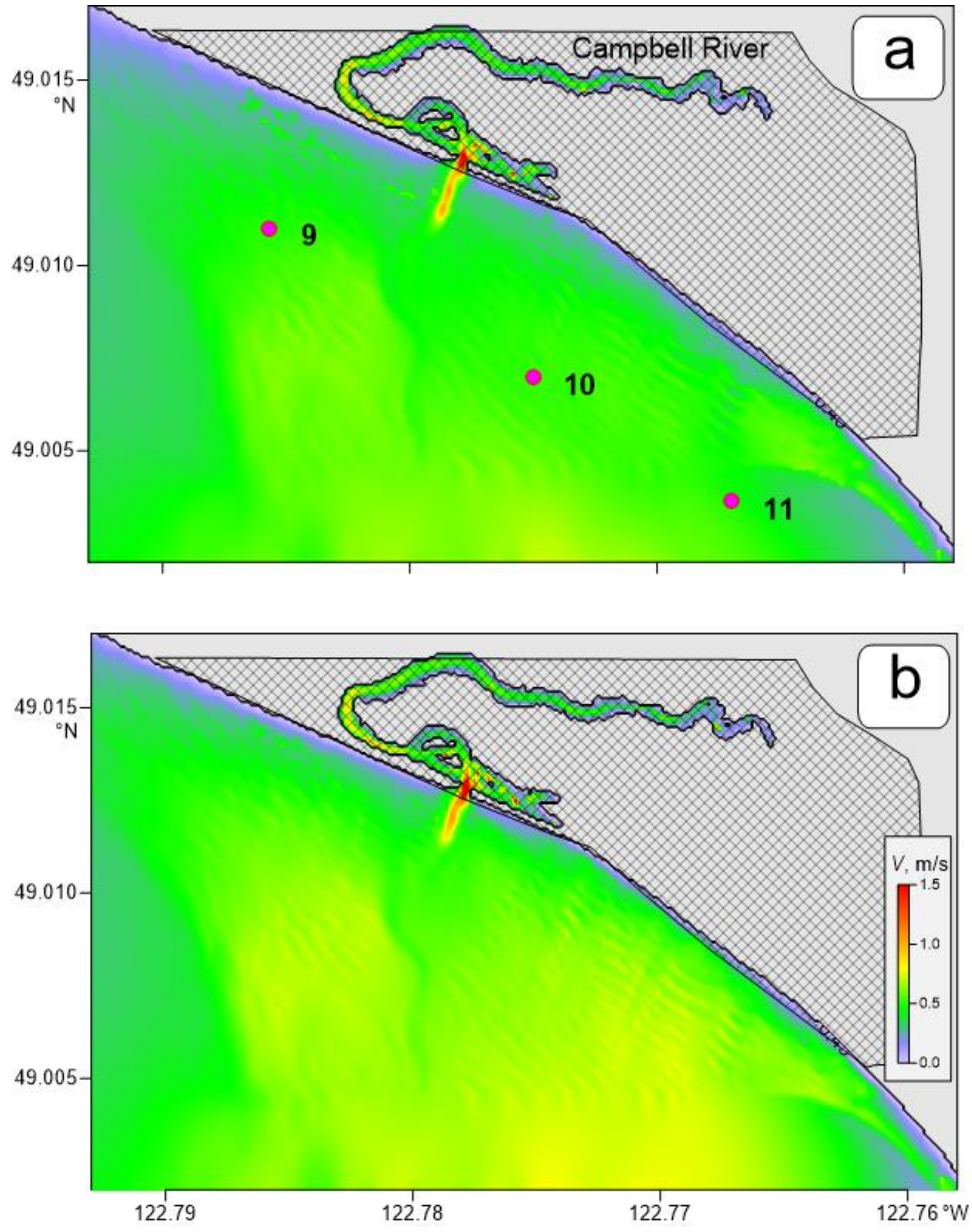

Figure 13. Distribution of maximum CSZ tsunami-induced currents (*V*, m/s) for Grid 4 for the Semiahmoo coast for (a) Model A and (b) Model B. Numbers in Boundary Bay denote sites for which tsunami wave records have been simulated.

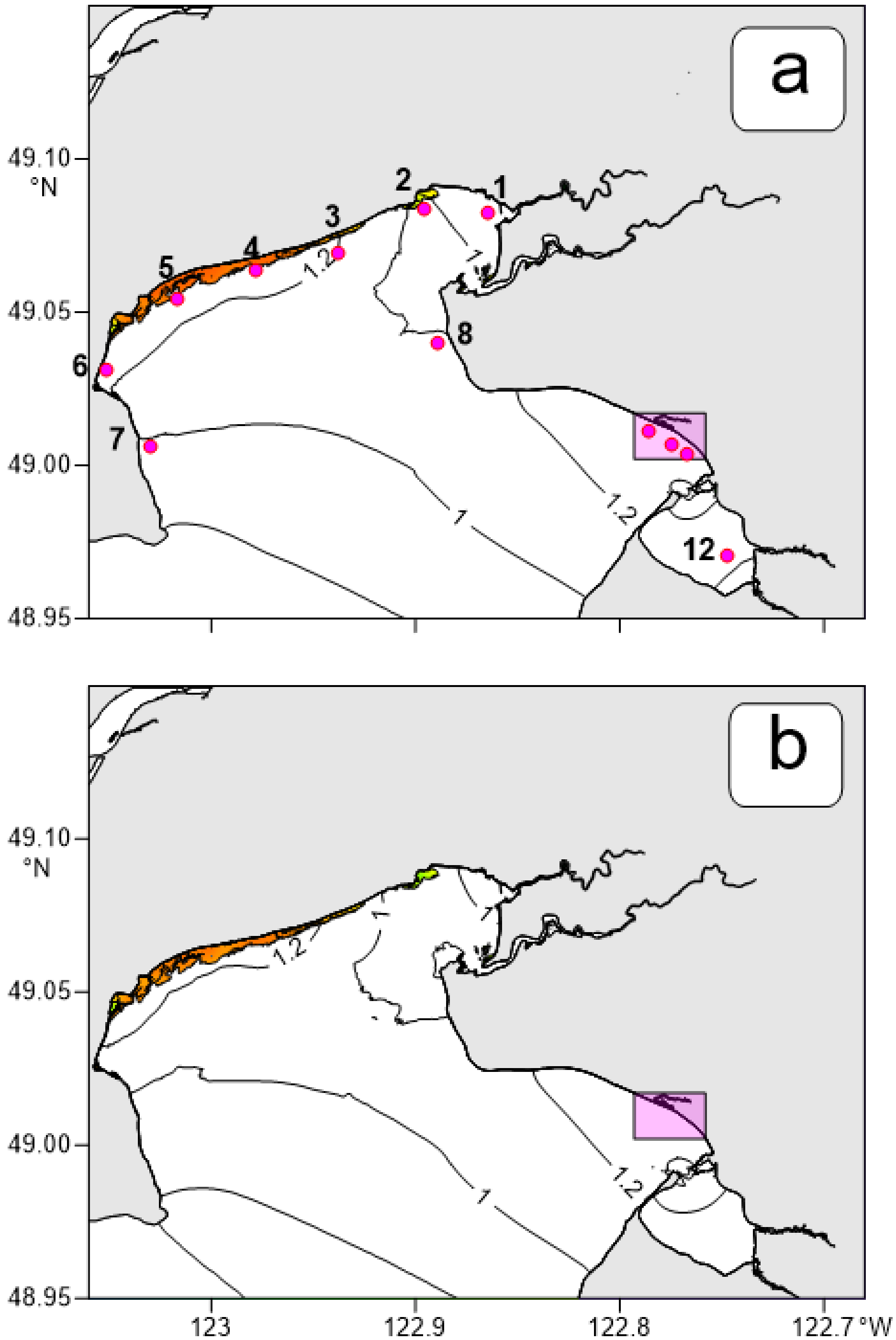

Figure 14. Map of the wave inundation area (in pink) in Boundary Bay during a CSZ tsunami for (a) Model A and (b) Model B. Initial conditions are Higher High Water Mean Tide. Numbers denote sites for which tsunami wave records have been simulated.

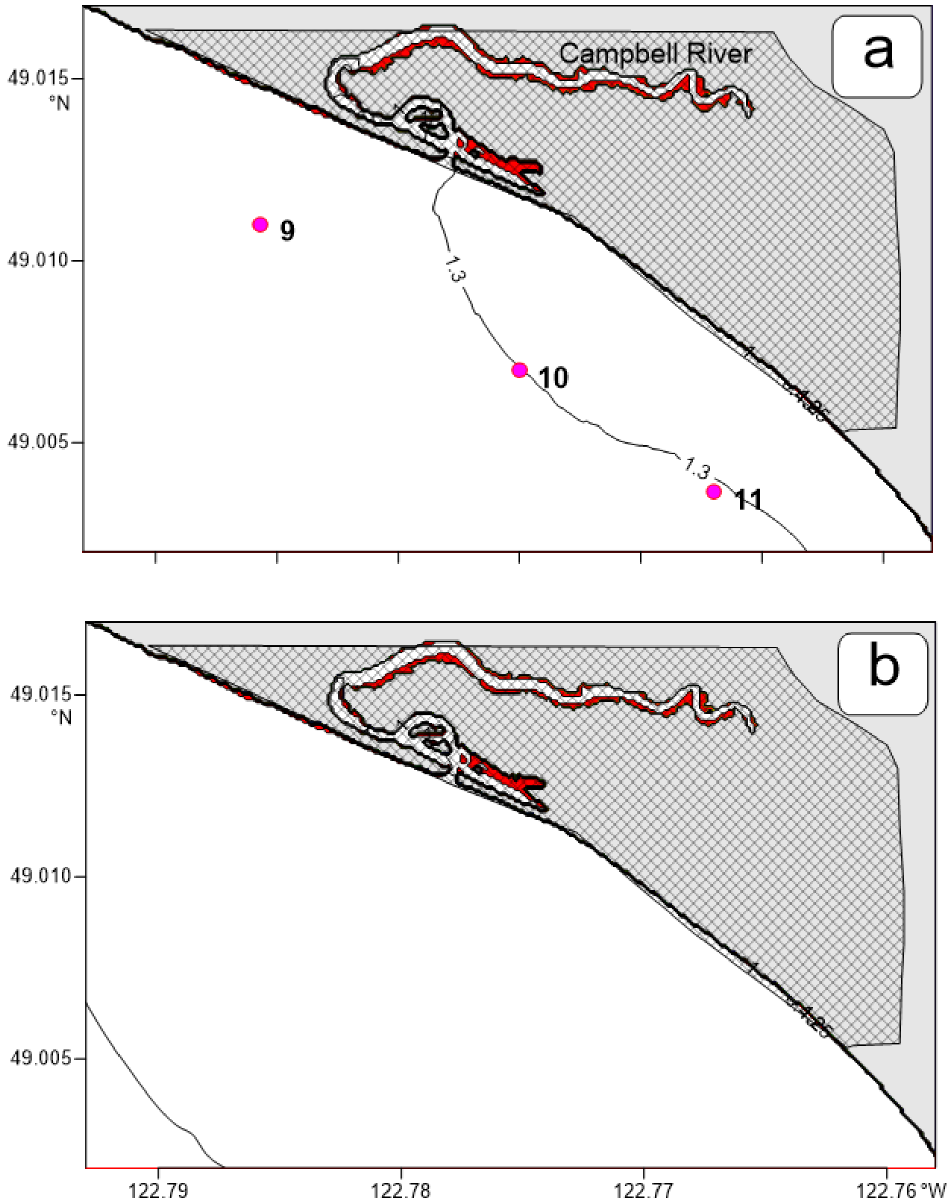

Figure 15. Map of the wave inundation area (in red) for the Semiahmoo First Nation region of Boundary Bay during a CSZ tsunami for (a) Model A and (b) Model B. Initial conditions are Higher High Water Mean Tide. Numbers denote sites for which tsunami wave records have been simulated.

Time series for Models A and B for the simulated waves and wave-induced currents at specific sites are presented in Figures 16 to 26; the statistical characteristics of these records are found in Tables 3-5. For each individual model run, the simulated wave amplitudes for Sites 1 to

7, located from east to west along the northern edge of Boundary Bay, the amplitude and time lag changes regularly. The wave first arrives at Site 7, then Site 6 and finally, Site 1. The wave amplitudes are greatest at the middle sites, Sites 4 and 5. Both models show similar results, with slightly lower amplitudes for Model B. For the sites at Semiahmoo (Site 9, Site 10 and Site 11, Figure 18), records are similar for both models. Wave amplitudes at the area are up to 1.3 m for both models, only marginally (less than by 2 %) higher for Model A. Records are started with a 70-75 cm trough with minimum at 2 h since earthquake, following by a higher crest, about 1.3 m at 2:40 after earthquake.

Table 3. Tsunami wave parameters for a Cascadia Subduction Zone tsunami at Boundary Bay for Model A numerical simulations. See Figures 10-11 for the site locations. Travel times for the maximum waves are in hours and minutes (HH:MM) after the start of the earthquake. Here, "displacement" of a wave crest or trough is measured relative to the still water level. Displacement is synonymous with amplitude in the case of a wave crest.

Site No	Highest crest		Deepest trough	
	Displacement (m)	Travel time HH:MM	Displacement (m)	Travel time HH:MM
1	1.15	03:14	-0.59	02:37
2	0.97	03:08	-0.68	02:26
3	1.19	03:00	-0.71	02:20
4	1.34	03:00	-0.22	02:14
5	1.30	03:02	-0.29	02:35
6	1.24	02:57	-0.65	02:10
7	0.99	02:47	-0.78	08:58
8	1.05	02:48	-0.80	08:58
9	1.28	02:43	-0.92	08:53
10	1.30	02:43	-1.01	08:55
11	1.30	02:44	-1.06	08:58
12	0.92	03:03	-0.67	02:19

Table 4. Tsunami wave parameters for a Cascadia Subduction Zone tsunami at Boundary Bay for the Model B numerical simulations. See Figures 10-11 for the site locations. Travel times for the maximum waves are in hours and minutes (HH:MM) after the start of the earthquake. "Displacement" of a wave crest or trough is measured relative to the still water level.

Site No	Highest crest		Deepest trough	
	Displacement (m)	Travel time HH:MM	Displacement (m)	Travel time HH:MM
1	1.07	03:10	-0.60	02:35
2	0.90	03:03	-0.69	02:24
3	1.15	02:56	-0.71	02:19
4	1.30	02:57	-0.22	02:11
5	1.25	02:59	-0.30	02:33
6	1.19	02:54	-0.65	02:08
7	0.96	02:42	-0.69	04:21
8	1.02	02:44	-0.72	02:01
9	1.27	02:39	-0.74	01:58
10	1.28	02:40	-0.82	08:54
11	1.28	02:49	-0.87	08:56
12	0.92	02:59	-0.68	02:18

Table 5. Wave-induced current speeds (*V*) for a Cascadia Subduction Zone tsunami in Boundary Bay for Models A and B numerical simulations. See Figures 10-11 for the site locations. The times for the occurrence of maximum wave-induced currents are in hours and minutes (HH:MM) after the start of the earthquake.

Site No	Model A		Model B	
	Maximum current speed (m/s)	Time of maximum current speed HH:MM	Maximum current speed (m/s)	Time of maximum current speed HH:MM
1	0.60	3:01	0.60	2:59
2	0.65	2:54	0.65	2:51
3	0.73	2:48	0.73	2:45
4	0.82	2:47	0.83	2:45
5	0.80	2:48	0.80	2:45
6	0.51	2:38	0.58	3:47
7	0.67	3:07	0.77	3:03
8	1.12	2:38	1.20	3:10
9	0.48	3:57	0.60	3:53
10	0.50	5:01	0.65	3:23
11	0.47	9:04	0.70	3:22
12	0.51	2:41	0.54	2:37

.

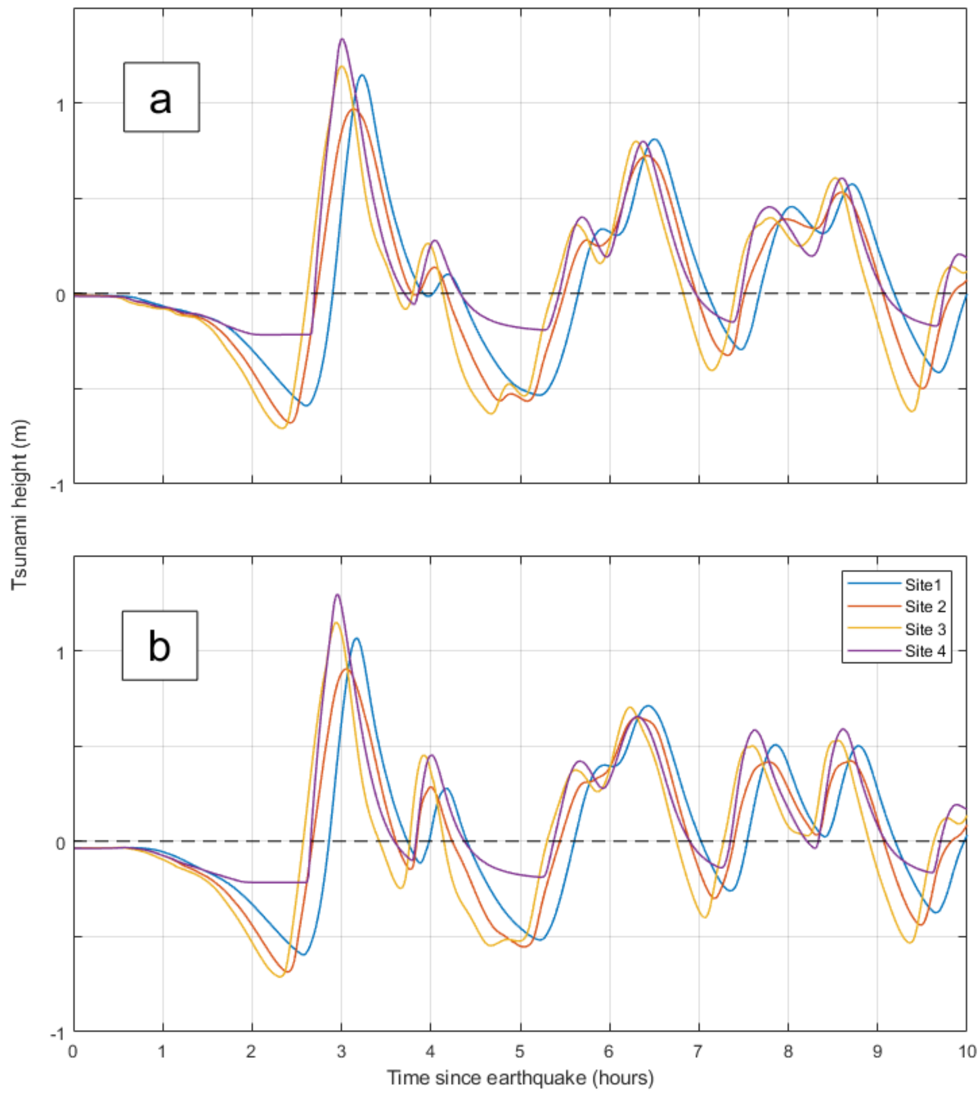

Figure 16. Simulated records of water level variations for a CSZ tsunami at Boundary Bay Sites 1, 2, 3 and 4 (See Figures 10-11 for the site locations) for (a) Model A; and (b) Model B.

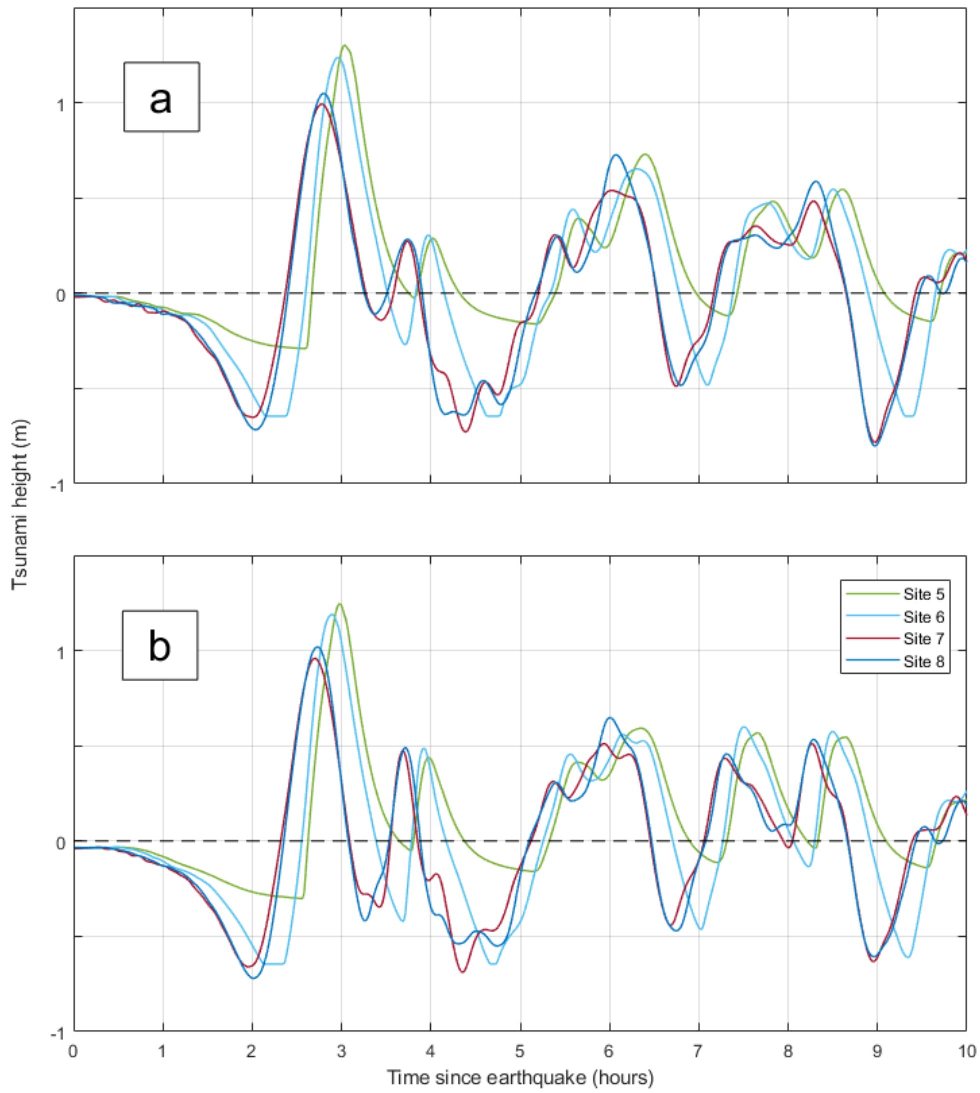

Figure 17. Simulated records of water level variations for a CSZ tsunami at Boundary Bay Sites 5, 6, 7 and 8 (See Figures 10-11 for the site locations) for (a) Model A; and (b) Model B.

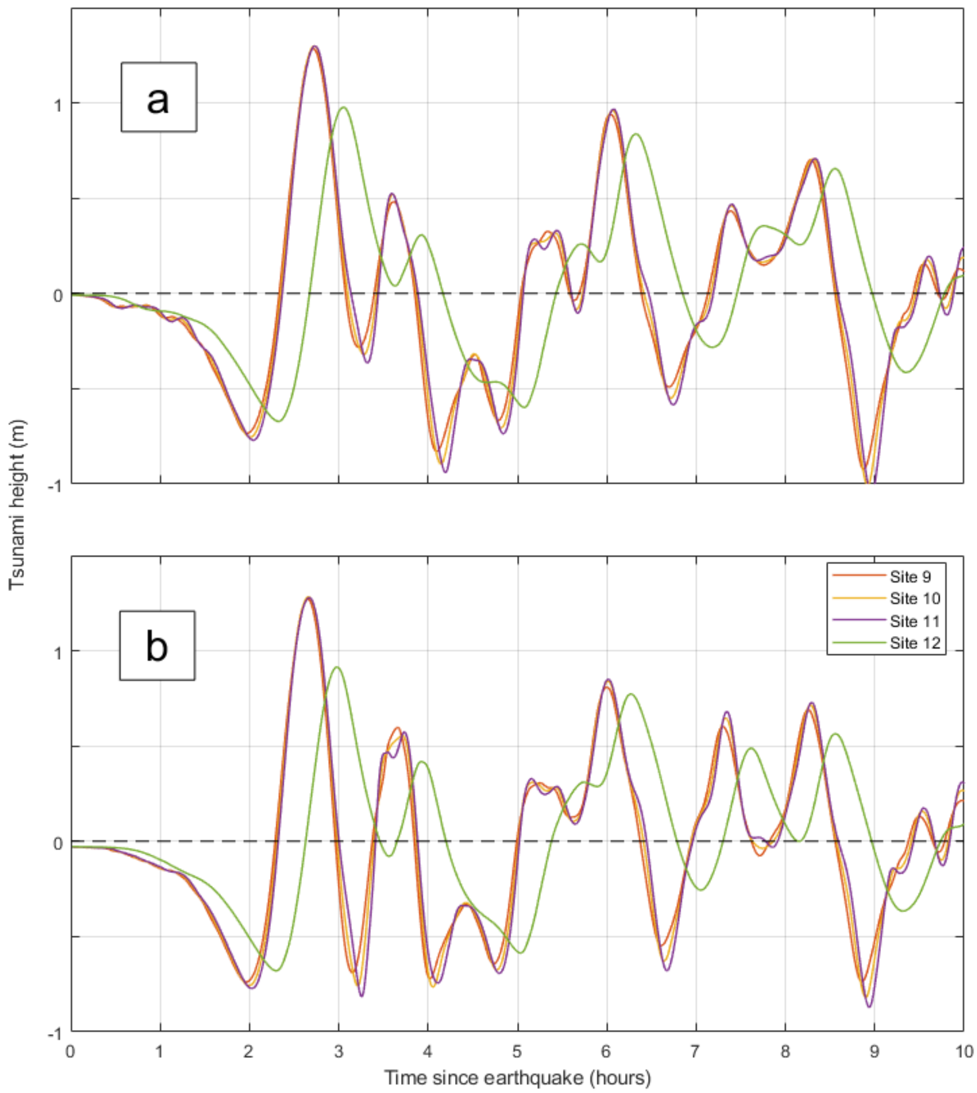

Figure 18. Simulated records of water level variations for a CSZ tsunami at Boundary Bay Sites 9, 10, 11 and 12 (See Figures 10-11 for the site locations) for (a) Model A; and (b) Model B.

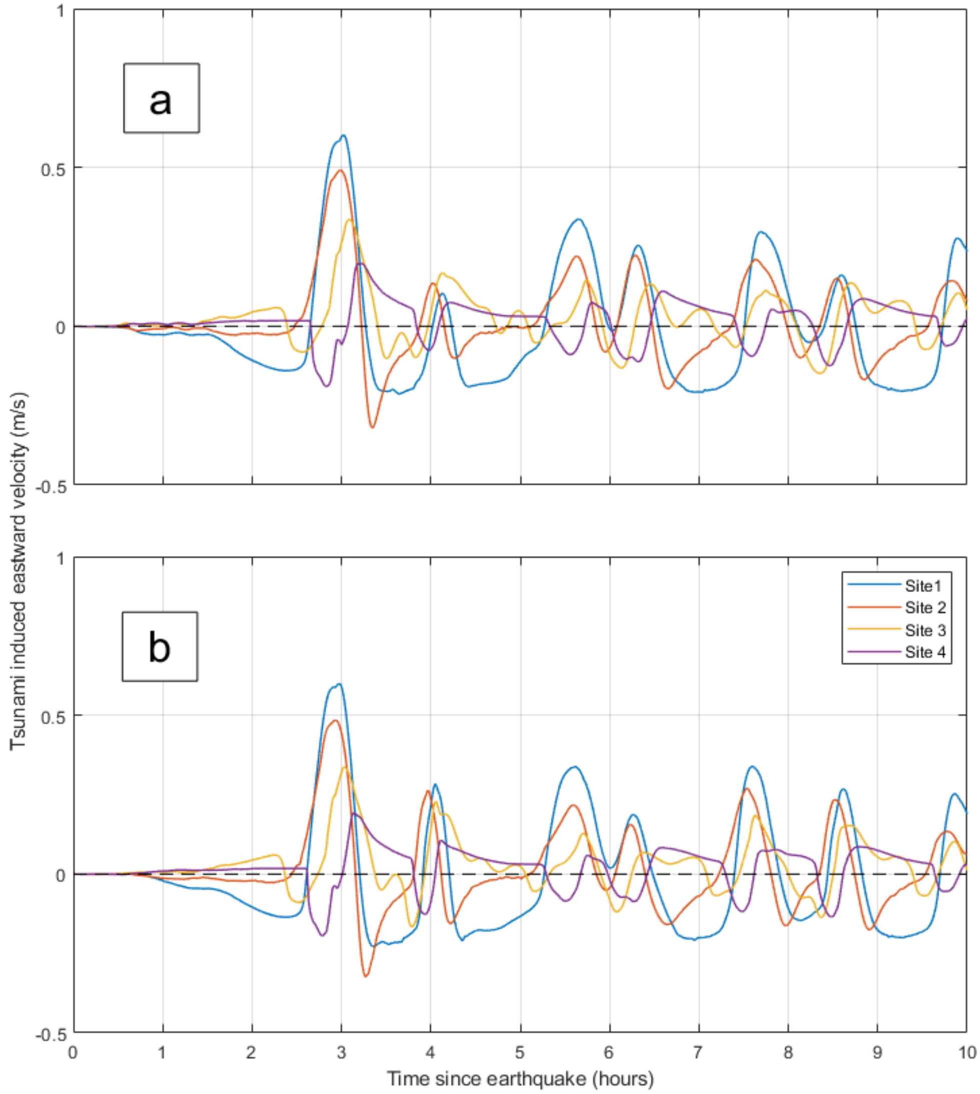

Figure 19. Simulated records of the eastward component of current velocity for a CSZ tsunami at Boundary Bay Sites 1, 2, 3 and 4 (See Figures 10-11 for the site locations) for (a) Model A; and (b) Model B.

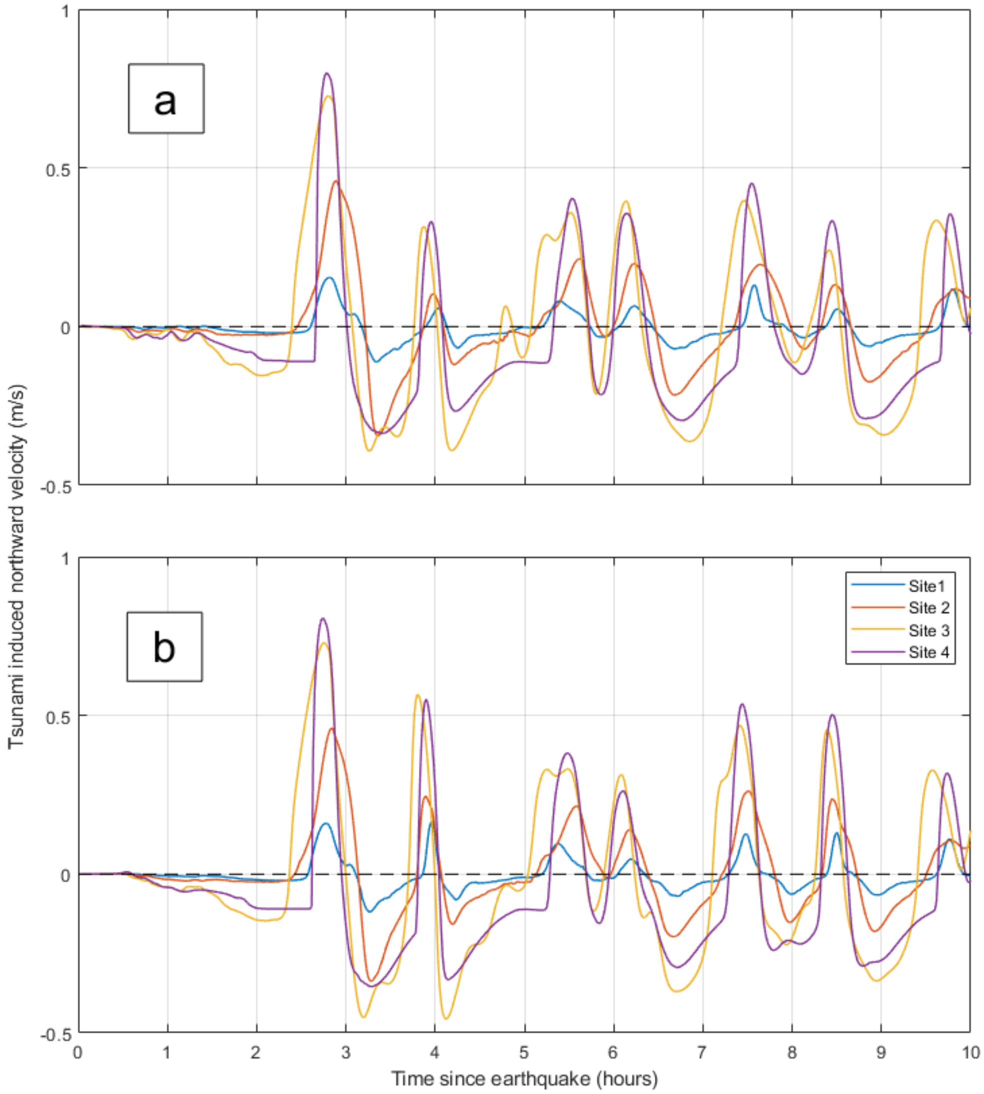

Figure 20. Simulated records of the northward component of current velocity for a CSZ tsunami at Boundary Bay Sites 1, 2, 3 and 4 (See Figures 10-11 for the site locations) for (a) Model A; and (b) Model B.

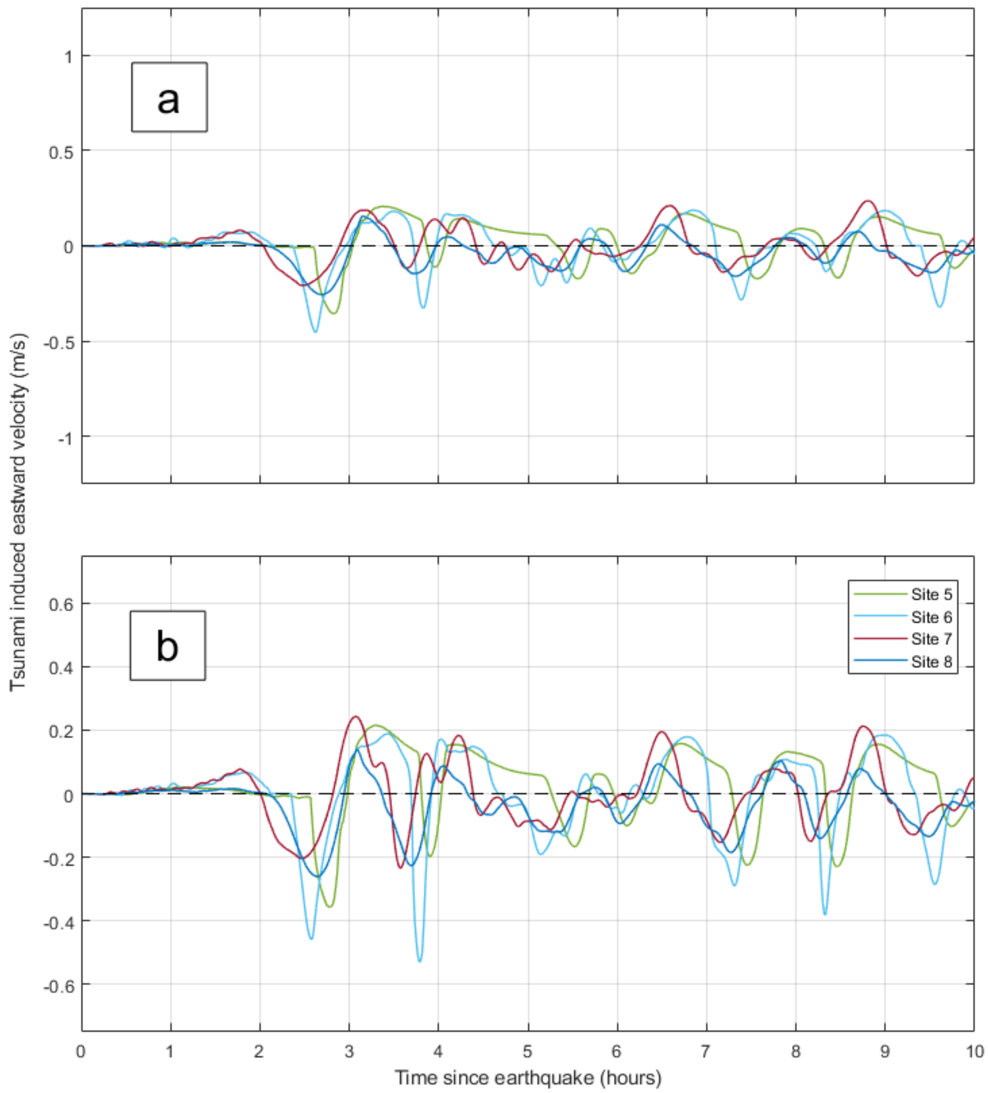

Figure 21. Simulated records of the eastward component of current velocity for a CSZ tsunami at Boundary Bay Sites 5, 6, 7 and 8 (See Figures 10-11 for the site locations) for (a) Model A; and (b) Model B.

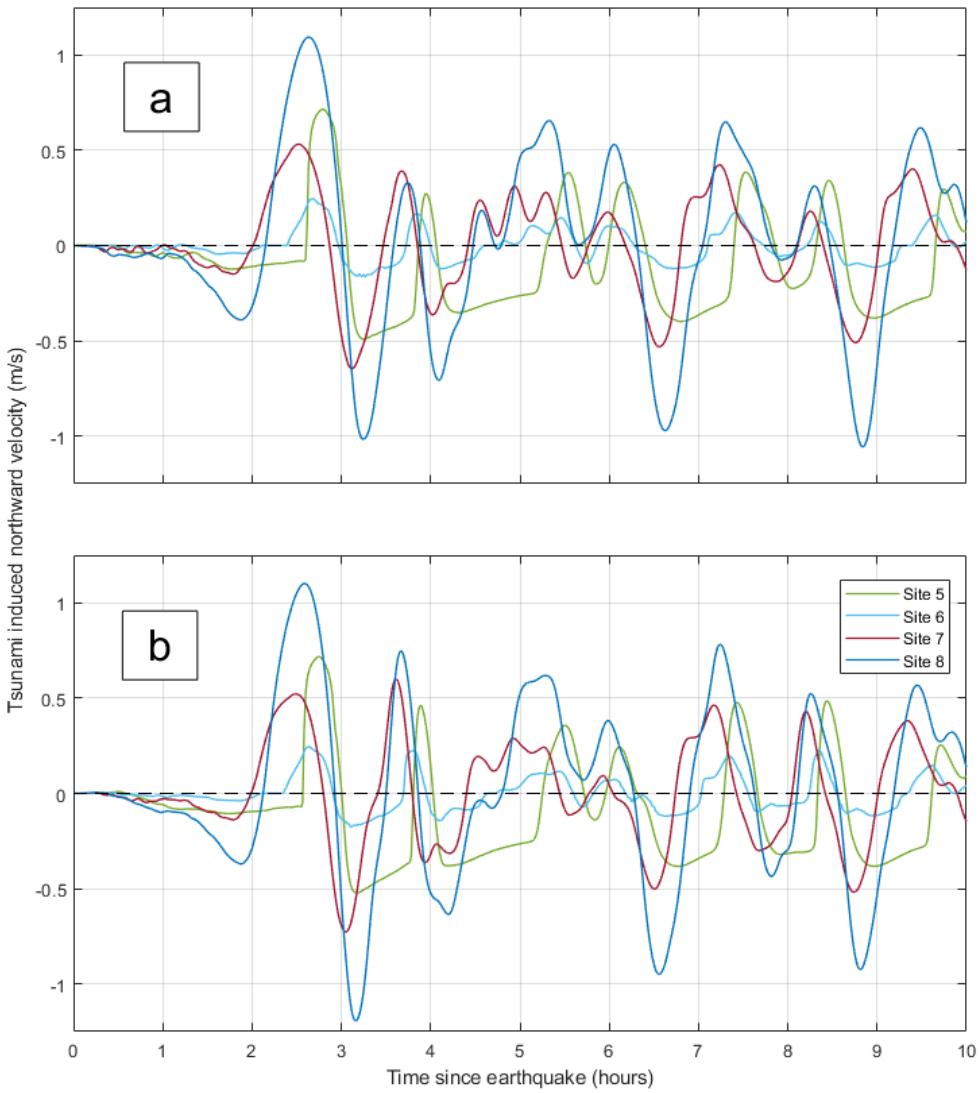

Figure 22. Simulated records of the northward component of current velocity for a CSZ tsunami at Boundary Bay Sites 5, 6, 7 and 8 (See Figures 10-11 for the site locations) for (a) Model A; and (b) Model B.

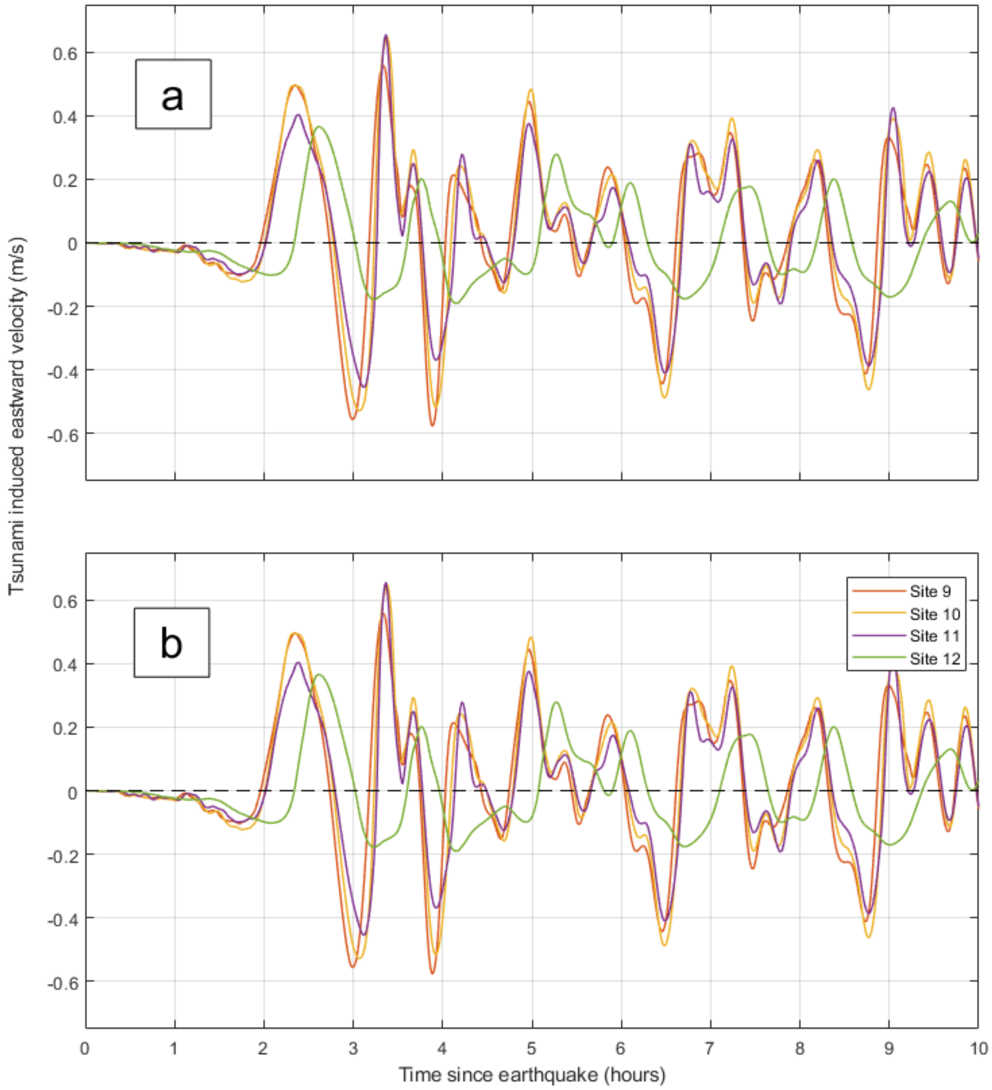

Figure 23. Simulated records of the eastward component of current velocity for a CSZ tsunami at Boundary Bay Sites 9, 10, 11 and 12 (See Figures 10-11 for the site locations) for (a) Model A; and (b) Model B.

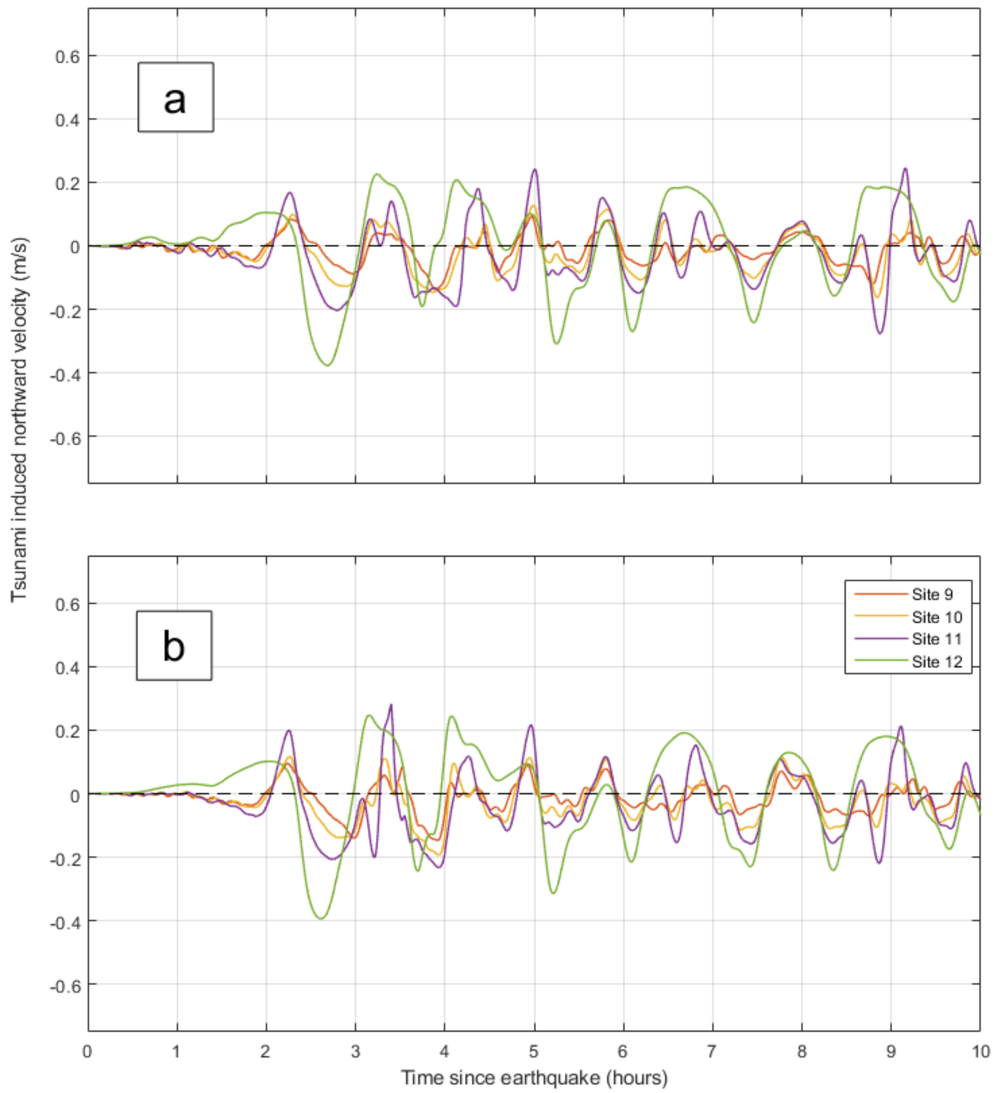

Figure 24. Simulated records of the northward component of current velocity for a CSZ tsunami at Boundary Bay Sites 9, 10, 11 and 12 (See Figures 10-11 for the site locations) for (a) Model A; and (b) Model B.

4. SUMMARY AND CONCLUSIONS

A high-resolution, four-level, nested-grid tsunami model was used to simulate tsunami waves and wave-induced currents that will be generated in Boundary Bay in the southern Strait of Georgia by a Cascadia Subduction Zone earthquake with magnitude M_w=9.0. Two versions of the earthquake-induced tsunami source region were used: Model A, a whole margin buried rupture; and Model B, a whole margin splay-faulting rupture. Both models started with sea level at the higher high water mean tide (HHWMT) level, and all results are computed relative to this vertical datum. The major results of the numerical modelling for the Boundary Bay area are:

- Models A and B produce similar results in Boundary Bay, Model A (the whole margin buried model) causes slightly higher (by 2-7%) wave amplitudes than the whole margin splay-faulting rupture scenario (Model B). Boundary Bay is more exposed to tsunami waves from a CSZ earthquake than the coast of Metro Vancouver.
- For both models, the first wave to arrive is a wave trough, with sea level dropping by 60-70 cm within 2-2.5 hours after the start of the earthquake.
- The leading wave crest that immediately follows the initial drop in water level is the highest wave. It reaches a peak of 1.1-1.5 m roughly 2:45 – 3:15 hours after the start of the earthquake.
- The major periods of tsunami waves in Boundary Bay and Semiahmoo Bay are 2-3 hours (dominant) and 1 hour (secondary, more pronounced in Model B).
- Wave amplitudes are distributed non-uniformly within Boundary Bay. Maximum wave amplitudes (of up to 1.5 m) occur within the north-western part on the Bay, and along the Semiahmoo coast (up to 1.3 m).
- The tsunami-induced ocean currents are typically less than 1 m/s in most areas, but are up to 3 m/s at the entrance to Drayton Harbor and up to 2 m/s at the mouth of Campbell River on the Semiahmoo coast. Model B produced slightly stronger currents than Model A.

- Tsunami waves would cause flooding, mostly in the north-western part of Boundary Bay. The flooding is restricted by the presence of the elongated dike along the northern coast of the bay. Flooding in the Semiahmoo area will likely occur in the Campbell River valley but will have a limited effect.

Although the modelling results indicate that the study region is not susceptible to major flooding from a CSZ tsunami, several limiting factors of the model need to be considered. Specifically, we have incomplete knowledge regarding the structure and vertical displacements associated with a future Cascadia Subduction Zone failure, and no knowledge of the ocean conditions at the time of a future earthquake. However, even if we add a 50% safety factor (a typical engineering value; cf. AECOM, 2013), the tsunami hazard to the Semiahmoo area remains confined to the low-lying regions along the Campbell River.

ACKNOWLEDGEMENTS

This project was funded through "Coastal Flood Mitigation Canada" within the Defence Research and Development Canada's Centre for Security Science (DRDC CSS) Program (CSSP), led on the Pacific Coast by the Geological Survey of Canada, Natural Resources Canada. We thank Marlene Jeffries (Canadian Hydrographic Service) and Mark Ranking (Ocean Networks, Canada) for providing us with the high-resolution bathymetric and topographic data for the Boundary Bay region and for helping with the vertical datum adjustment.

REFERENCES

AECOM (2013), *Modelling of Potential Tsunami Inundation Limits and Run-Up, Capital Regional District*, Project No. 6024 2933, 36 p.

British Columbia 3 arc-second Bathymetric Digital Elevation Model (2017). https://www.ngdc.noaa.gov/metaview/page?xml=NOAA/NESDIS/NGDC/MGG/DEM/iso/xml/4956.xml&view=getDataView&header=none

Cherniawsky, J.Y., Titov, V.V., Wang, K., and Li, J.-Y. (2007), Numerical simulations of tsunami waves and currents for southern Vancouver Island from a Cascadia megathrust earthquake, *Pure and Applied Geophysics* 164 (2-3), 465-492, doi:10.1007/s00024-006-0169-0.

Eungard D.W., Forson C., Walsh T.J., Gica E, and Arcas D. (2018). Tsunami Hazard maps of the Anacortes-Bellingham area, Washington – model results from a ~2500-year Cascadia Subduction Zone earthquake scenario. Washington Geological Survey, Map series 2018-2, June 2018.

Fine I.V., Thomson, R.E., Lupton, L.M., and Mundschutz, S. (2019a). *Numerical Modelling of a Cascadia Subduction Zone Tsunami at the Canadian Coastal Base at Seal Cove, British Columbia.* Unpublished Report, Institute of Ocean Sciences, Sidney, BC.

Fine I.V., Thomson, R.E., Lupton, L.M., and Mundschutz, S. (2019b). *Numerical Modelling of a Cascadia Subduction Zone Tsunami at the Canadian Coastal Base at Victoria, British Columbia.* Unpublished Report, Institute of Ocean Sciences, Sidney, BC.

Gao, D. (2016). *Defining Megathrust Tsunami Sources at Northernmost Cascadia Using Thermal and Structural Information*. Master of Science Thesis, School of Earth and Ocean Sciences, The University of Victoria, Victoria, BCm https://dspace.library.uvic.ca/handle/1828/7435

GEBCO (The General Bathymetric Chart of the Oceans), http://www.gebco.net/, Last access on November 20,2016.

Leonard, L.J., Rogers, G.C., and Mazzotti, S. (2014), Tsunami hazard assessment of Canada, *Natural Hazards*, 70, 237-274.

National Tsunami Hazard Mapping Program (NTHMP) (2010). *Guidelines and best practices for tsunami inundation modeling for evacuation planning*. NTHMP Mapping & Modeling Subcommittee, NOAA,USA.

Suleimani, E.N., Nicolsky, D.J., and Koehler, R.D. (2013). *Tsunami Inundation Maps of Sitka, Alaska.* Report of Investigations 2013-3, State of Alaska, Department of Natural Resources, Division of Geological and Geophysical Surveys, Fairbanks, AK, 76 p., 1 sheet, scale 1:250,000. doi: 10.14509/26671.

The City of Prince Rupert Tsunami Flood Risk Assessment (2019). Prepared by Northwest Hydraulic Consultants Ltd for City of Prince Rupert. http://www.princerupert.ca/sites/default/files/services/public%20safety/20190621%203003349%20Prince%20Rupert%20Tsunami%20Report.pdf

Thomson, R. E. and Emery, W. J. (2014). *Data Analysis Methods in Physical Oceanography*. 3rd Edition. Elsevier Science, Amsterdam, London, New York, 716 p.

Wang, K., and Tréhu, A.M. (2016), Invited review paper: Some outstanding issues in the study of great megathrust earthquakes—The Cascadia example, *Journal of Geodynamics*, 98, 1-18.

Witter, R.C., Zhang, Y.J., Wang, K., Priest, G.R., Goldfinger, C., Stimely, L., English, J.T., and Ferro, P.A. (2013), Simulated tsunami inundation for a range of Cascadia megathrust earthquake scenarios at Bandon, Oregon, USA, *Geosphere*, 9 (6), 1783-1803, doi:10.1130/GES00899.1